JIMMA UNIVERSITY

SCHOOL OF GRADUATE STUDIES

JIMMA INTITUTE OF TECHNOLOGY

FACULITY OF CIVIL AND ENVIRONMENTAL ENGINEERING

STRUCTURAL ENGINEERING STREAM

Shear Strengthening of Reinforced Concrete Beam by Embedded Connector Steel Plate

Msc Thesis

A thesis Submitted to School of Graduate Studies of Jimma University in Partial Fulfillment of the Requirements for the Degree of Masters of Science in Structural Engineering

By:

NIGATU SOLOMON

AUGUST, 2020

JIMMA, ETHIOPIA

JIMMA UNIVERSITY

SCHOOL OF GRADUATE STUDIES

JIMMA INSTITUTE OF TECHNOLOGY

FACULTY OF CIVIL AND ENVIROMENTAL ENGINEERING

STRUCTURAL ENGINEERING STREAM

Shear Strengthening of Reinforced Concrete Beam by Embedded Connector Steel Plate

A thesis Submitted to School of Graduate Studies of Jimma University in Partial Fulfillment of the Requirements for the Degree of Masters of Science in Structural Engineering

By: Nigatu Solomon

ADVISOR: ENGR. ELMER.C. AGON (ASSO. PROF.)

CO-ADVISOR: ENGR. ABINET ALEMSEGED

AUGUST, 2020

JIMMA, ETHIOPIA

DECLARATION

This thesis entitled "*Shear Strengthening of Reinforced Concrete Beam by Embedded Connector Steel Plate"* is my original work and has not presented for a degree in this and any other university. I have not previously in its entirely or in part submitted it for obtaining any qualification. All sources of material used in this work have been duly acknowledged.

NAME: Nigatu Solomon

Signature: ______________

Date: 02/08/2020

ENGR. ELMER.C. AGON (Asso. Prof.)	______________	02/08/2020
Advisor	Signature	Date
ENGR. ABINET ALEMSEGED	______________	02/08/2020
Co-advisor	Signature	Date

JIMMA UNIVERSITY

SCHOOL OF GRADUATE STUDIES
JIMMA INSTITUTE OF TECHNOLOGY
FACULTY OF CIVIL AND ENVIRONMENTAL ENGINEERING
STRUCTURAL ENGINEERING CHAIR

SHEAR STRENGTHENING OF REINFORCED CONCRETE BEAM BY EMBEDDED CONNECTOR STEEL PLATE

NIGATU SOLOMON

APPROVED BY BOARD OF EXAMINERS

1. Eng. Elmer C. Agon	______________	02/ 08/ 2020
Main Advisor	Signature	Date
2. Eng. Abinet Alemseged	______________	02/ 08/ 2020
Co-Advisor	Signature	Date
3. Dr. Binaya Patnaik	______________	02/ 08/ 2020
External Examiner	Signature	Date
4. Eng. Y, Anand Yenemula	______________	02/ 08/ 2020
Internal Examiner	Signature	Date
5. Engr. Diosdado John Corpuz	______________	02/ 08/ 2020
Chairman	Signature	Date

ACKNOWLEDGMENT

I am sincerely thankful to have the opportunity and pleasure to work with my advisors Engr. Elmer.C.Agon and Engr. Abinet Alemseged. They provide significant help making this research.

I gratefully acknowledge the bodies which funded this research. These are: Jimma University, Jimma Institute of Technology and Ethiopian Road Authority Sponsorship.

Lastly, I would like to thank my family for all their support and being with me until the completion of the thesis.

ABSTRACT

Many concrete structures fail to provide the specific needs due to change in the design standards, unexpected loading, corrosion, design and construction errors and due to random loading in the form of earthquakes. Damaged structures are to be replaced or retrofitted. Shear in the beam is primarily resisted by the stirrups provided as shear reinforcement. Beam members with insufficient stirrup bars require retrofitting in shear critical region, in order to enhance their shear strength.

Different shear strengthening technique are provided using steel plates from this near surface mounted steel plate is one of them and the main drawback is debonding of the plate which is solved using embedded connector steel plate. The aim of this research is to investigate the shear resistance of reinforced concrete beam using embedded connector steel plates and to investigate the performances of shear-strengthened beams through numerical investigations.

Shear strengthening of beams were done by providing additional embedded connector steel plate along the shear span of a beam using different connector depth and width of steel plate. A total of ten beams were modeled. All the beams have the same dimensions and reinforcement details. The beams were designed intentionally to fail in shear. The relative efficiency of the various strengthening steel plate width and connector depth were examined.

The result of this research showed that the width of steel plate had great contribution on the shear strength by increasing the bond between concrete and plates. The connector depth also had a contribution by providing stiffness to the section. W30D200 had failure load increment 36.22% compared to control beam. The embedded connector of shear-strengthened beam of proposed design based on failure load (W30D200) had shown shear failure with higher failure load and maximum ductile nature.

It was recommended that since strengthening using embedded steel plate is economical, resisted debonding of plates and had a positive effect on shear strengthening of concrete beam future studies should considered.

Keywords: *shear strengthening, embedded connector, steel plate, failure load*

TABLE OF CONTENTS

DECLARATION I

ACKNOWLEDGMENT II

ABSTRACT III

TABLE OF CONTENTS IV

LIST OF FIGURES VII

LIST OF TABLES IX

ACRONYMS X

CHAPTER ONE 1

INTRODUCTION 1

1.1 Background of the Study 1

1.2 Statement of the Problem 2

1.3 Objective of the Study 3

1.3.1 General Objective 3

1.3.2 Specific Objectives 3

1.4 Scope and Limitations of the Study 3

CHAPTER TWO 4

RELATED LITERATURE REVIEW 4

2.1 Strengthening of Structures 4

2.2 Strengthening for Shear 4

2.3 Different shear strengthening techniques using plates 5

2.4 Concrete Damaged Plasticity Model 6

2.4.1 Uniaxial tension and compression stress behavior 6

2.4.2 Defining tension stiffening 8

2.5 Shell elements 10

2.5.1 Element geometry 10
2.5.2 Conventional shell versus continuum shell 10
CHAPTER THREE 12
RESEARCH METHODOLOGY 12
3.1 Research Design 12
3.1.1 Description of Reference Test specimen for validation Md. Ashraful Alam *et al.* (2017) 12
3.1.2 Description of Specimen 14
3.2 Study Variables 16
3.3 Finite element modeling 16
3.3.1Geometric modeling 17
3.3.2 Material modeling 17
3.3.3 Finite element mesh 22
3.3.4 Interaction 24
3.3.4 Boundary conditions 24
3.4 Loading and Interpretation of Results 25
CHAPTER FOUR 26
RESULT AND DISCUSSION 26
4.1 Validation of Finite Element Analysis 26
4.1.1 Numerical Analysis Using ABAQUS 27
4.2 Finite Element Analysis output 29
4.2.1 Load Carrying Capacity 29
4.2.2 Failure mode 31
4.2.3 Load versus Deflection 33
CHAPTER FIVE 39

CONCLUSIONS AND RECOMMENDATIONS 39

5.1 Conclusions 39

5.2 Recommendations 40

REFERENCES 41

APPENDICES 44

Appendix A: Design of beam 44

Appendix B: Input file for a reference CB model 47

LIST OF FIGURES

Figure 2.1 Response of concrete to uniaxial loading in (a) tension and (b) compression 8

Figure 2.2 Illustration of the definition of the cracking strain $\boldsymbol{\varepsilon tck}$ used for the definition of tension stiffening data. 9

Figure 2.3 Conventional versus continuum shell element. 11

Figure 3.1 Shear strengthening of RC beam using steel plate and embedded connector: (a) surface preparation with hole of connector; (b) embedded connector; (c) prepared surface and connector for strengthening; (d) shear-strengthened beam. 13

Figure 3.2 Longitudinal section (a) Control Beam (b) Specimens 15

Figure 3.3 Cross section (a) control beam (b) 25 mm depth connector (c) 50 mm depth connector (d) 200 mm depth connector 16

Figure 3.4 Compression Stress-Strain relation for concrete 18

Figure 3.5 Tensile Stress-Strain relation for concrete 19

Figure 3.6 Tensile stress verses crack opening relation... 20

Figure 3.7 Tensile stress - strain relation for C20/25 concrete 21

Figure 3.8 Stress and crack opening relation for C20/25 concrete 21

Figure 3.9 Stress strain relation for reinforcing steel and steel plate 22

Figure 3.10 Element mesh, (a) mesh for control beam, (b) mesh for beams with steel plate....... 23

Figure 3.11 Boundary condition 25

Figure 4.1 BSC20 beam a) Model, b) Mesh and c) Deflection result 28

Figure 4.2 Failure mode (a) CB, (b) W20D25, (c) W25D25, (d)W30D25, (e) W20D50, (f)W25D50, (g)W30D50, (h)W20D200, (i)W25D200, (j)W30D200, ... 33

Figure 4.3 Load deflection curve for 25mm connector depth 34

Figure 4.4 Load deflection curve for 50mm connector depth 35

Figure 4.5 Load deflection curve for 200mm connector depth 35

Figure 4.6 Effect of embedded connector depth, (a) for steel plate width 20mm, (b) for steel plate 25mm and (c) for steel plate 30mm 37

Figure 4.7 Load deflection curve for hole effect 38

LIST OF TABLES

Table 3-1 Details of specimen 14

Table 3-2 CDP parameter 18

Table 4-1 Summary of Results from Journal, All Beams 26

Table 4-2 Comparison with journal result 29

Table 4-3 Failure load 30

Table 4-4 Failure mode 31

ACRONYMS

CDP	Concrete damaged plasticity
d_c	Compression damage variable
d_t	Tension damage variable
E_{cm}	Secant modulus of the concrete
E_0	Initial (undamaged) elastic stiffness of the material
Es	Elastic modulus of steel
f_{cm}	Mean compressive strength of concrete
F_{ctm}	Mean tensile strength of concrete
FRP	Fiber reinforced plate
f_y	Yield strength of reinforcing steel
G_f	Fracture energy
RC	Reinforced concrete
V_c	Shear resistance capacity of concrete
V_{plate}	Shear resistance of plates
$V_{plateed\ beam}$	Shear resistance of plated beam
W	Crack displacement
W_c	Critical crack opening displacement
ε_c	Compression strain
ε_s	Strain of steel at any point

ε_t	Tension strain
$\tilde{\varepsilon}_t^{ck}$	Cracking strain
$\tilde{\varepsilon}_c^{pl}$	Compression equivalent plastic strains
$\tilde{\varepsilon}_t^{pl}$	Tension equivalent plastic strains
$\dot{\tilde{\varepsilon}}_c^{pl}$	Compression equivalent plastic strain rates
$\dot{\tilde{\varepsilon}}_t^{pl}$	Tension equivalent plastic strain rates
θ	Temperature
σ_c	Compression stress
σ_t	Tension stress
σ_{cu}	Ultimate stress,
σ_{c0}	Initial yield stress
σ_{t0}	Failure stress
$\bar{\sigma}_c$	Compressive cohesion stress
$\bar{\sigma}_t$	Tensile cohesion stress

CHAPTER ONE

INTRODUCTION

1.1 Background of the Study

Structural members are subjected to shear and flexural loads. Mainly RC beams are designed to have a higher shear capacity than flexural capacity, so shear failure can be avoided as it is brittle and sudden in nature.

Many concrete structures fail to provide the specific needs due to change in the design standards, unexpected loading, corrosion, design and construction errors and due to random loading in the form of earthquakes. Damaged structures are to be replaced or retrofitted. Shear in the beam is primarily resisted by the stirrups provided as shear reinforcement. Beam members with insufficient stirrup bars require retrofitting in shear critical region, in order to enhance their shear strength.

Upgrading of existing structures has emerged as one of the major construction activities all over the world today. Upgrading of existing structures becomes necessity due to various reasons; some of those are change in design codes and deterioration with time due to environmental effects. Design codes are constantly being upgraded in many countries including Ethiopia as new loading requirement dictates for higher strengths demanded of structural members.

In the recent years, the performance of RC structures was upgraded using different technique and materials. The advancement of new materials and technologies has led researchers to investigate various designs and materials to increase the strength of shear critical RC beams [1–7]. One of those materials was steel plates; many researches were conducted on the externally bonded steel plates for FRP composites [8-11], natural fiber plates and aluminum alloy plates [12, 13]. Strengthening with other material has a drawback on cost effectiveness. But strengthening using steel plates has an advantage which is cost effective and reliable material [14]. In many research works shear strengthening of rectangular RC beams with steel plate applied using three different techniques: full wrapping, U-wrapping, and side strips. Full wrapping provides the highest effectiveness followed by U-wrapping on the shear strengthening of RC beams and had drawback on the application for those flanged section which had walls and slabs. However, side-bonded strips are the most practical to apply where it does not need access to the top or the bottom of the beam. The main disadvantage of side strip steel plates is deboning of plates where it is caused by concrete cracks leading to the separation of the adhesive from concrete surface at ends of strengthening plate. Many numerical models were produced; little has been done toward modeling mechanical anchor like the embedded connector. This research was conducted to fill a gap on the premature deboning of side plates by embedded connector used to strengthening shear critical rectangular RC beams.

Finite elements analysis helps understand the behavior of retrofitted beam members effectively and economically. Many studies were carried out to justify the validity of modeling and analysis of structural members using ABAQUS. Conclude that this nonlinear finite element software has an advantage to stress and deflections at the centered are compared well to the experimental data’s.

In this study, the effect of connector depth was studied to determine the efficient width for steel plate, using nonlinear structural software called ABAQUS.

1.2 Statement of the Problem

RC beams are designed to have a higher shear capacity than flexural capacity, so shear failure can be avoided as it is brittle and sudden in nature. However, multiple causes such as severe corrosion of the steel stirrups due to deterioration or change in loading can lead to lower shear capacity.

The Ethiopian building code standard has been revised after two decades. The new design code has emerged with increased peak ground acceleration passing. And the existing structures are inadequate due to the increment of in peak ground acceleration (change in loading). So our societies always call to researchers to give good and effective solutions of rehabilitation inadequate existing structures in shear capacity.

This study provides an effective solution to risk associated with brittle failure of existing structures which is an urgent issue and a great concern of our society about the safety of the existing infrastructures particularly buildings.

1.3 Objective of the Study

1.3.1 General Objective

The main objective of this study is to strengthen shear capacity of reinforced concrete beams using embedded connector steel plate.

1.3.2 Specific Objectives

More specifically, the study has the following objective: -

- To determine the most efficient size/width of steel plate
- To determine the effect of drilled holes on concrete strength
- To determine effect of connector depth

1.4 Scope and Limitations of the Study

This study conducted only on slender beams with internal force of flexure and shear. Deep beams, beam-columns, Pre-stressed beams and beams made of high-strength concrete, numbers of connector in a single plate, different dimensions of connector, different arrangement of steel plates were not covered in the investigation.

CHAPTER TWO

RELATED LITERATURE REVIEW

2.1 Strengthening of Structures

Upgrading of existing infrastructures has emerged as one of the major construction activities all over the world today. Upgrading of existing structures becomes necessity due to various reasons; some of those are revised design code and deterioration with time due to environmental effects. The existing concrete structures have required strengthening or stiffening in order to increase their ultimate flexural or shear capacity, or to control deflections and cracking. [15] Design codes are constantly being upgraded in many countries as new loading requirement dictates for higher strengths demanded of structural members. Numerous concrete structures constructed in the past in countries like USA and Japan do not meet current seismic design codes especially concerning shear capacity and ductility. The Hyogoken–Nanbu Earthquake in 1995 caused tremendous damage to concrete structures in Japan. Several reinforced concrete piers and rigid frames, used for elevated highways were severely damaged during this earthquake. The failure pattern showed insufficient shear capacity and lack of ductility in piers and main beams of these structures [16].

Similarly, in Ethiopia a new design code has been released. This revision of code was done for the higher strength demand of structures. Earth quake parameters and empirical formulas of shear resistance were changed in the revised code.

2.2 Strengthening for Shear

Reinforced concrete structures are designed to fail by flexure and also the amounts of flexural reinforcement have limits to ensure ductile failure and give warring for occupant. But shear failure is sudden and brittle. Generally, in the design of RC beams, this failure type should be avoided. Therefore, existing structures should be highly checked for their shear strength capacity. Design codes have been continually improved but structural failures have result from inadequacies in design for shear [15].

It is accepted, however, that in a reinforced concrete beam the shear force is carried by a combination of: concrete in the compression zone; aggregate interlock; dowel action and shear reinforcement (if provided). The factors that affect the shear strength of a reinforced concrete beam are: concrete properties; beam size; beam shape and reinforcement details. There are three basic shear failure types, dependent upon shear span to depth ratio can be categorized as: deep beam failure; shear compression and diagonal tension. In Ethiopia, the shear empirical formulas of shear resistance were changed in the revised design code. Generally, both the empirical formulas of shear resistance concrete and web reinforcement in these old and revised design codes were different. The variation of both design codes in shear resistance concrete was depending mainly on compressive strength concrete. During the construction if construction errors are occurred and due to the environmental effect the shear strength of RC members are decreased. There for those structures needs upgrading in the shear resistance of the section.

2.3 Different shear strengthening techniques using plates

In the recent years, the performance of RC structures was upgraded using different technique and materials. The advancement of new materials and technologies has led researchers to investigate various designs and materials to increase the strength of shear critical RC beams [1–7]. One of those materials was steel plates; many researches were conducted on the externally bonded steel plates for FRP composites [8-11], natural fiber plates and aluminum alloy plates [12, 13]. Strengthening with other material has a drawback on cost effectiveness. But strengthening using steel plates has an advantage which is cost effective and reliable material [14]. In many research works shear strengthening of rectangular RC beams with steel plate applied using three different techniques: full wrapping, U-wrapping, and side strips. Full wrapping provides the highest effectiveness followed by U-wrapping on the shear strengthening of RC beams and had drawback on the application for those flanged section which had walls and slabs. However, side-bonded strips are the most practical to apply where it does not need access to the top or the bottom of the beam. The main disadvantage of side strip steel plates are deboning of plates where it is caused by concrete cracks leading to the separation of the adhesive from concrete surface at ends of strengthening plate. Many numerical models were produced; little has been done toward modeling mechanical anchor like the embedded connector.

The potential disadvantages of other strengthening techniques using steel plate bonding are as follows:

• *Cost of plates*: They are more expensive than steel plates of the equivalent load capacity. However, the difference between the two materials is likely to be reduced as production volumes and competition between manufacturers' increases. Comparison of total contract costs for alternative methods of strengthening will be based on labour and access costs as well as material costs.

• *Mechanical damage*: They are more susceptible to damage than steel plates and could be damaged by a determined attack, such as with an axe. In vulnerable areas with public access, the risk may be removed by covering the plate bonding with a render coat, plate may be cut out over the damaged length, and a new plate bonded over the top with an appropriate lap. [17]

2.4 Concrete Damaged Plasticity Model

CDP is continuum, plasticity-based, damage model for concrete. It assumes that the main two failure mechanisms are tensile cracking and compressive crushing of the concrete material. The evolution of the yield (failure) surface is controlled by two hardening variables, $\tilde{\varepsilon}_t{}^{pl}$ and $\tilde{\varepsilon}_c{}^{pl}$, linked to failure mechanism under tension and compression loading, respectively.

2.4.1 Uniaxial tension and compression stress behavior

The model assumes that the uniaxial tensile and compressive response of concrete is characterized by damaged plasticity, as shown in **Figure 2.1**. Under uniaxial tension the stress-strain response follows a linear elastic relationship until the value of the failure stress,σ_{t0} is reached. The failure stress corresponds to the onset of micro-cracking in the concrete material. Beyond the failure stress the formation of micro-cracks is represented macroscopically with a softening stress-strain response, which induces strain localization in the concrete structure. Under uniaxial compression the response is linear until the value of initial yield stress, σ_{c0}, In the plastic regime the response is typically characterized by stress hardening followed by strain softening beyond the ultimate stress, σ_{cu}. This representation, although somewhat simplified, captures the main features of the response of concrete.

It is assumed that the uniaxial stress-strain curves can be converted into stress versus plastic-strain curves. (This conversion is performed automatically by ABAQUS from the user-provided stress versus “inelastic” strain data, as explained below.) Thus,

$$\sigma_t = \sigma_t(\tilde{\varepsilon}_t{}^{pl}, \dot{\tilde{\varepsilon}}_t{}^{pl}, \theta, f_i) \qquad 2.1$$

$$\sigma_c = \sigma_c\left(\tilde{\varepsilon}_c{}^{pl}, \dot{\tilde{\varepsilon}}_c{}^{pl}, \theta, f_i\right) \qquad 2.2$$

Where the subscripts t and c refer to tension and compression, respectively; $\tilde{\varepsilon}_t{}^{pl}$ and $\tilde{\varepsilon}_c{}^{pl}$ are the equivalent plastic strains, $\dot{\tilde{\varepsilon}}_t{}^{pl}$ and $\dot{\tilde{\varepsilon}}_c{}^{pl}$ are the equivalent plastic strain rates, θ is the temperature, and $f_i, (i = 1, 2, \dots)$are other predefined field variables.

As shown in **Figure 2.1**, when the concrete specimen is unloaded from any point on the strain softening branch of the stress-strain curves, the unloading response is weakened: the elastic stiffness of the material appears to be damaged (or degraded). The degradation of the elastic stiffness is characterized by two damage variables, d_t and d_c, which are assumed to be functions of the plastic strains, temperature, and field variables:

$$d_t = d_t\left(\tilde{\varepsilon}_t{}^{pl}, \theta, f_i\right);\ 0 \le d_t \le 1, \qquad 2.3$$

$$d_c = d_c\left(\tilde{\varepsilon}_c{}^{pl}, \theta, f_i\right);\ 0 \le d_t \le 1. \qquad 2.4$$

The damage variables can take values from zero, representing the undamaged material, to one, which represents total loss of strength.

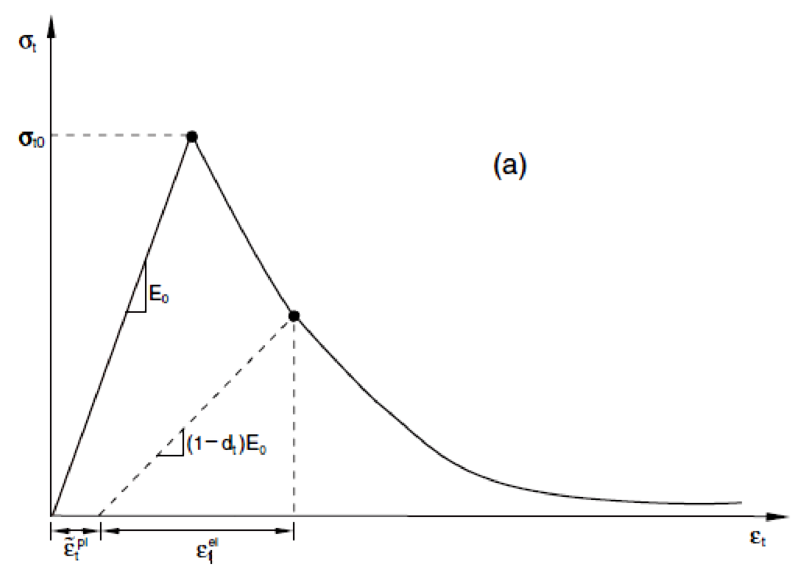

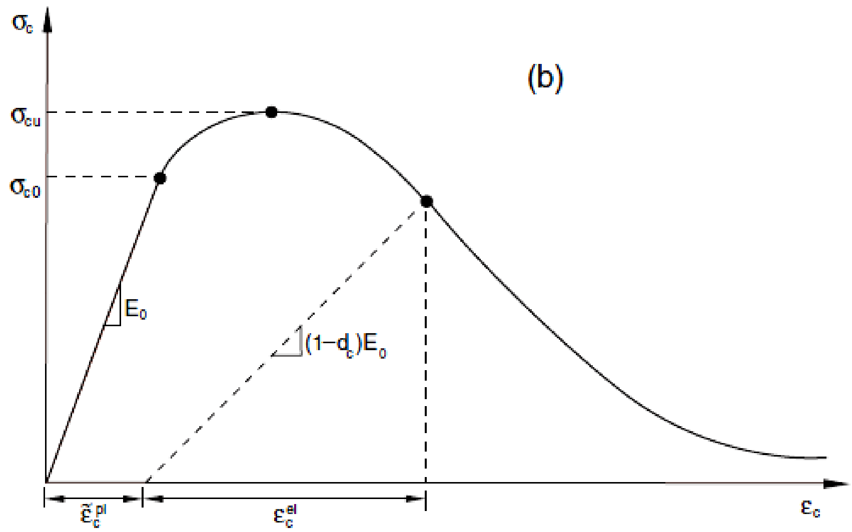

Figure 2.1 Response of concrete to uniaxial loading in (a) tension and (b) compression

If E_0 is the initial (undamaged) elastic stiffness of the material, the stress-strain relations under uniaxial tension and compression loading are, respectively [18]:

$$\sigma_t = (1 - d_t)E_0\left(\varepsilon_t - \tilde{\varepsilon}_t{}^{pl}\right), \tag{2.5}$$

$$\sigma_c = (1 - d_c)E_0\left(\varepsilon_c - \tilde{\varepsilon}_c{}^{pl}\right). \tag{2.6}$$

The "effective" tensile and compressive cohesion stresses expressed as

$$\bar{\sigma_t} = \frac{\sigma_t}{(1-d_t)} = E_0\left(\varepsilon_t - \tilde{\varepsilon}_t{}^{pl}\right), \tag{2.7}$$

$$\bar{\sigma_c} = \frac{\sigma_c}{(1-d_c)} = E_0\left(\varepsilon_c - \tilde{\varepsilon}_c{}^{pl}\right),, \tag{2.8}$$

2.4.2 Defining tension stiffening

The post-failure behavior for direct straining is modeled with tension stiffening, which allows you to define the strain-softening behavior for cracked concrete. This behavior also allows for the effects of the reinforcement interaction with concrete to be simulated in a simple manner. Tension stiffening is required in the concrete damaged plasticity model. Tension stiffening can specify by means of a post-failure stress-strain relation or by applying a fracture energy cracking criterion.

2.4.2.1 Post-failure stress-strain relation

In reinforced concrete the specification of post-failure behavior generally means giving the post-failure stress as a function of cracking strain. $\tilde{\varepsilon}_t{}^{ck}$. The cracking strain is defined as the total strain minus the elastic strain corresponding to the undamaged material; that is, $\tilde{\varepsilon}_t{}^{ck} = \varepsilon_t - \varepsilon_{0t}{}^{el}$, where $\varepsilon_{0t}{}^{el} = {}^{\sigma_t}/_{E_0}$, as illustrated in **Figure 2.2**. To avoid potential numerical problems, ABAQUS enforces a lower limit on the post-failure stress equal to one hundred of the initial failure stress: $\sigma_t \geq {}^{\sigma_{t0}}/_{100}$.

Tension stiffening data are given in terms of the cracking strain, $\tilde{\varepsilon}_t{}^{ck}$. ABAQUS automatically converts the cracking strain values to plastic strain values using the relationship

$$\tilde{\varepsilon}_t{}^{pl} = \tilde{\varepsilon}_t{}^{ck} - \frac{d_t}{(1-d_t)}\frac{\sigma_t}{E_0} \quad , \qquad 2.9$$

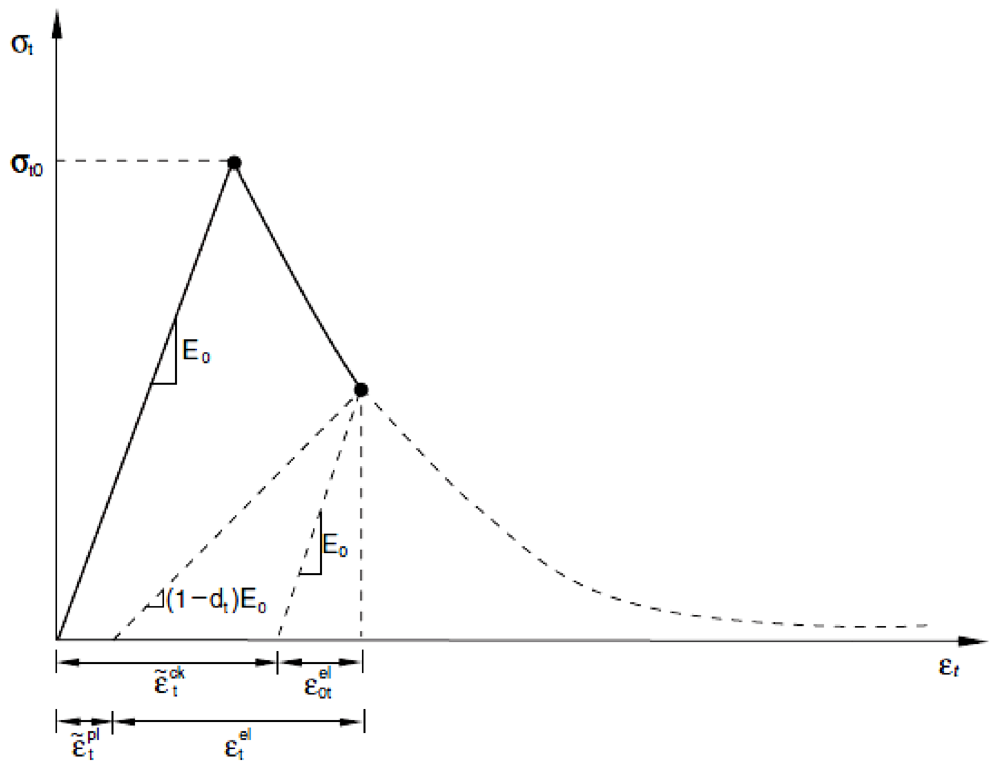

Figure 2.2 Illustration of the definition of the cracking strain $\tilde{\boldsymbol{\varepsilon}}_t{}^{\boldsymbol{ck}}$ used for the definition of tension stiffening data.

2.5 Shell elements

To use shell element, one dimension (the thickness) is significantly smaller than other dimension and in which the stress in the thickness direction are negligible. A structure whose thickness is less than 1/10 of global structural dimension generally can be modeled with shell elements.

2.5.1 Element geometry

Two types of shell elements are available in Abaqus: conventional shell elements and continuum shell elements. Conventional shell elements discretize a reference surface by defining the element's planar dimensions, its surface normal, and its initial curvature. The nodes of a conventional shell element, however, do not define the shell thickness; the thickness is defined through section properties. Continuum shell elements, on the other hand, resemble three-dimensional solid elements in that they discretize an entire three-dimensional body yet are formulated so that their kinematic and constitutive behavior is similar to conventional shell elements. Continuum shell elements are more accurate in contact modeling than conventional shell elements, since they employ two-sided contact taking into account changes in thickness. For thin shell applications, however, conventional shell elements provide superior performance [19].

2.5.2 Conventional shell versus continuum shell

Shell elements are used to model structures in which one dimension, the thickness, is significantly smaller than the other dimensions. Conventional shell elements use this condition to discretize a body by defining the geometry at a reference surface. In this case the thickness is defined through the section property definition. Conventional shell elements have displacement and rotational degrees of freedom.

In contrast, continuum shell elements discretize an entire three-dimensional body. The thickness is determined from the element nodal geometry. Continuum shell elements have only displacement degrees of freedom. From a modeling point of view continuum shell elements look like three-dimensional continuum solids, but their kinematic and constitutive behavior is similar to conventional shell elements [20].

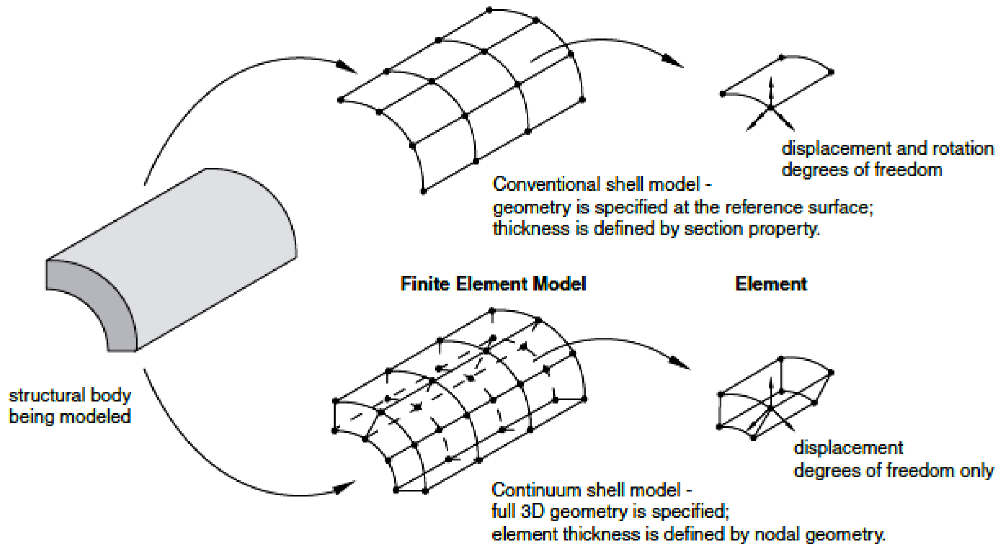

Figure 2.3 Conventional versus continuum shell element.

CHAPTER THREE

RESEARCH METHODOLOGY

3.1 Research Design

In this research methodology, first the accuracy of the modeling techniques was checked by preparing the same sample with the reference test specimen using ABAQUS. The specimens in this research were prepared, and material provided were checked based on the requirement of EBCS EN 1994-1-1:2013. The width and thickness of steel plate were chosen based on the design approach recommended on EBCS EN 1994-1-1:2013 for the shear links. All beams were modeled on nonlinear finite element analysis software ABAQUS 6.14-1 and the output were discussed on the result and discussion parts.

3.1.1 Description of Reference Test specimen for validation Md. Ashraful Alam *et al.* (2017)

In**.** Ashraful Alam *et al.* research four beams with dimensions of 150mm× 300mm× 2300 mm were fabricated. The beams were grouped into group CB (control beam) and group BSC (beam steel plate with connector). Group CB consisted of one control beam Group BSC consisted of three beams, which were BSC20, BSC25, and BSC30. The width of the shear strip plates was selected based on the proposed theoretical models. Beams BSC20 and BSC30 were designed based on tensile and yield strength of shear link and designed widths of plates were 20mm and 30 mm, respectively. Beam BSC25 was prepared based on arbitrary basis, and the width of the plate was 25 mm. The thickness of all strengthening plates was 2.75 mm. The embedded connector system was applied with a hole of 20 mm, 25 mm, and 30mm diameter, respectively, and steel bars with diameters of 16 mm, 16 mm, and 20mm were inserted into the holes, respectively, in order to eliminate premature debonding failure. The plates were spaced with 130mm spacing and applied only on the shear critical spans.

The concrete cube compressive strength used for the casting of beams was 31.385 MPa. A 16mm steel bar was used for main reinforcement with yield strength of 548 MPa and tensile strength of 620 MPa, while 6mm bar was used for shear link with yield strength of 305 MPa and tensile strength of 458 MPa. Steel plates with yield strength of 275 MPa and tensile strength of 320 MPa were used for shear strengthening.

The surface of the beam was roughened in the targeted areas to remove the weak concrete cover and loose particles in order to apply the adhesive on a concrete surface with sufficient strength as the concrete cover would fail at low loads shown in the following Figure

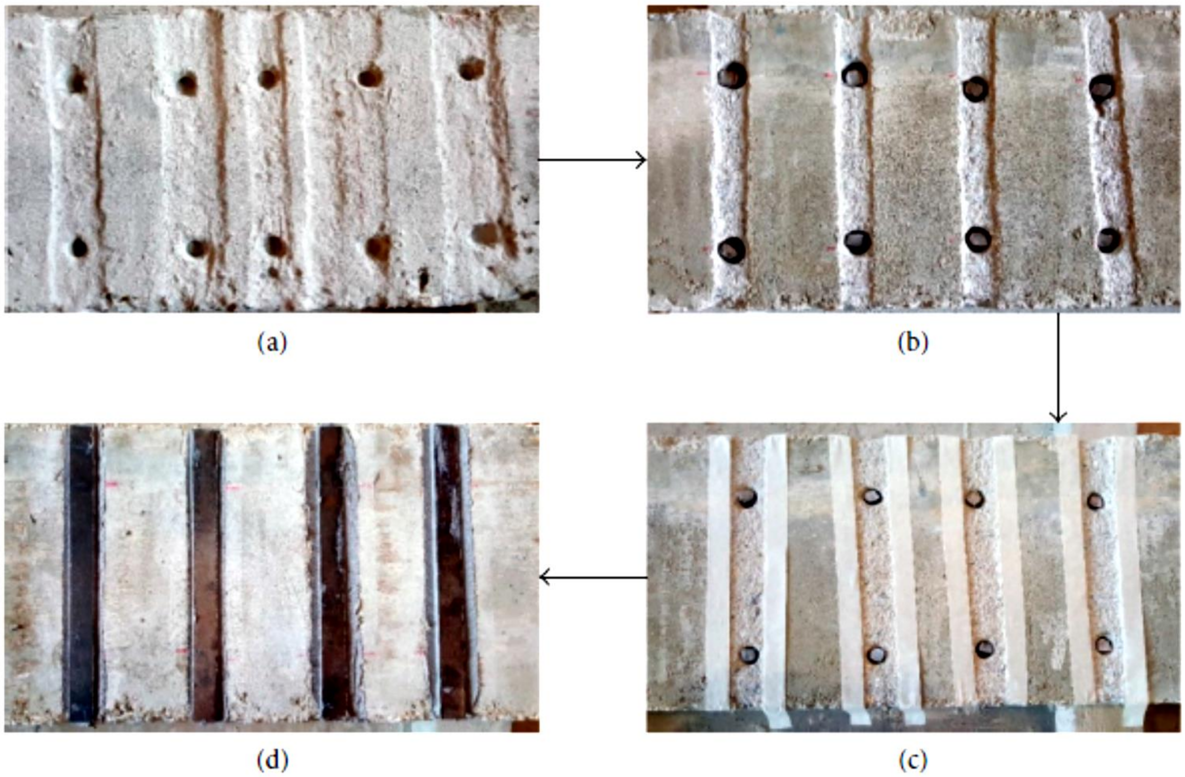

Figure 3.1 Shear strengthening of RC beam using steel plate and embedded connector: (a) surface preparation with hole of connector; (b) embedded connector; (c) prepared surface and connector for strengthening; (d) shear-strengthened beam.

In connector system, two holes with a depth of 21–24mm and the specified diameter were drilled in the roughened area of each steel plate at the distance of 50mm from the lower and upper edges of the beam. Epoxy resin (Sikadur-30) was used to all the holes of the connectors, and then, pieces of steel bars of the specified diameter and 21 mm–24mm in length were placed into the adhesive-filled drilled holes.

Steel plates were fixed on the sides of the beams by epoxy resin and embedded connector system. The epoxy resin was spread in 3mm layer over the roughened area on the concrete beam, and the steel plate was applied with firm pressure to ensure proper bonding with no air voids. Epoxy resin was left until it completely dried out, and disruption was avoided. [21]

3.1.2 Description of Specimen

Shear strengthening of beams were done by providing additional embedded connector steel plate along the shear span of a beam using different connector depth and width of the plate. A total of ten beams were modeled using ABAQUS 6.14-1. All the beams have the same dimensions and reinforcement details. The beam has a width of 200 mm, depth of 250 mm and overall length of 1700 mm. The beams were reinforced and detailed as shown in below. All beams were designed intentionally to fail in shear. In all beams there was no shear reinforcement internally. C20/25 concrete grade is used. The yield strength and elastic modulus of longitudinal reinforcement were 500 MPa and 200 GPa respectively. The yield strength of 250MPa is used for the steel plate, and a diameter of 16mm bar with 500MPa yield strength of connector were considered.

Connector depth 25mm, 50mm and 200mm were selected based on the width of the beam, the first was at depth of cover to reinforcement (1/8 width of beam), next depth was ¼ width of beam and the last one was full width of beam. Steel plate was provided on the shear critical regions with 120mm spacing. Spacing of steel plate was calculated using the conventional shear link design and shear to flexural load ratio were used in this research to determine the different width of steel plate. Additional three beams were modeled to determine the effect of the hole prepared to embed the connector on the shear capacity of the beam. the diameter and the depth of the hole was the same as the size of embedded connectors.

Table 3-1 Details of specimen

Specimen	Steel plate dimension			Embedded connector	
	Length (mm)	Width (mm)	Thickness (mm)	Diameter (mm)	Depth (mm)
CB	-	-	-	-	-
W20D25	250	20	3	16	25
W25D25	250	25	3	16	25
W30D25	250	30	3	16	25
W20D50	250	20	3	16	50
W25D50	250	25	3	16	50
W30D50	250	30	3	16	50
W20D200	250	20	3	16	200
W25D200	250	25	3	16	200
W30D200	250	30	3	16	200

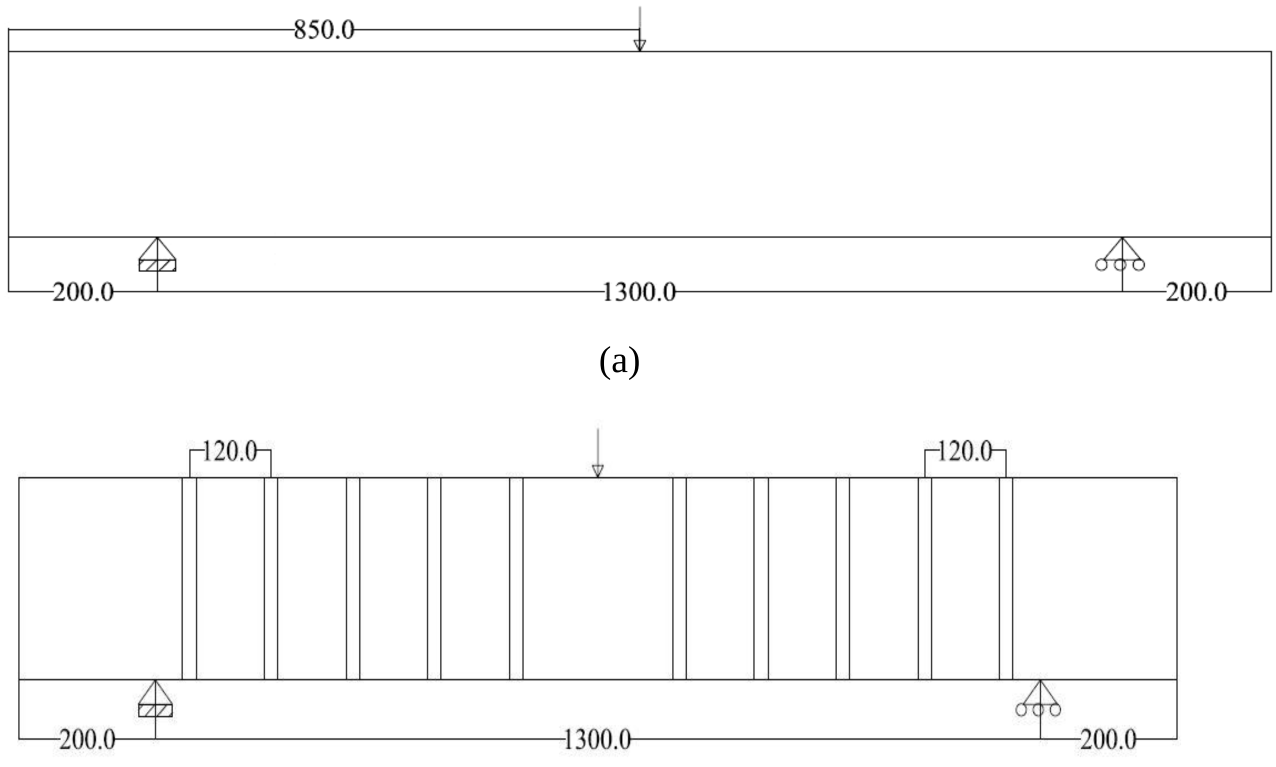

(a) (b)

Figure 3.2 Longitudinal section (a) Control Beam (b) Specimens

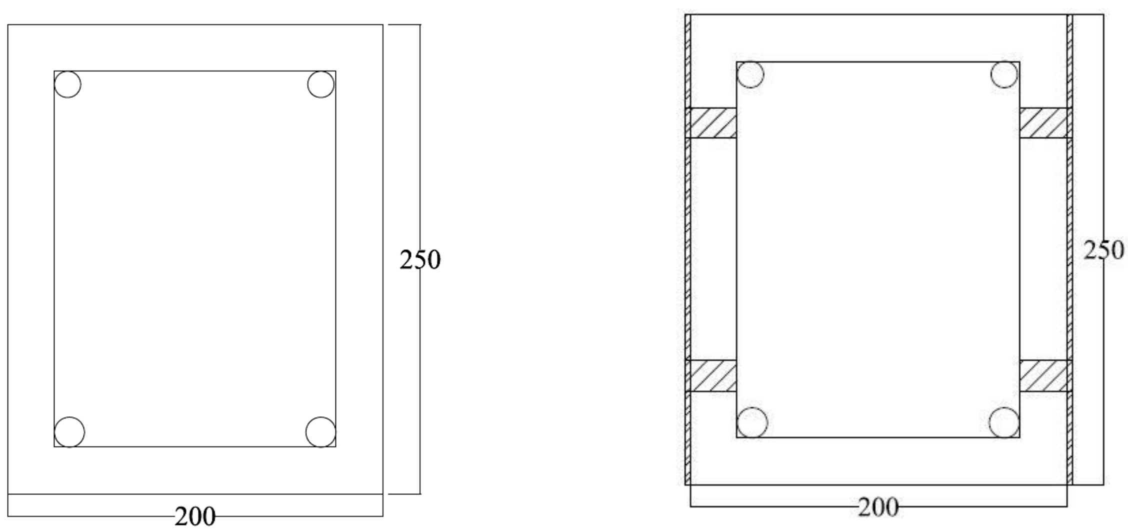

(a) (b)

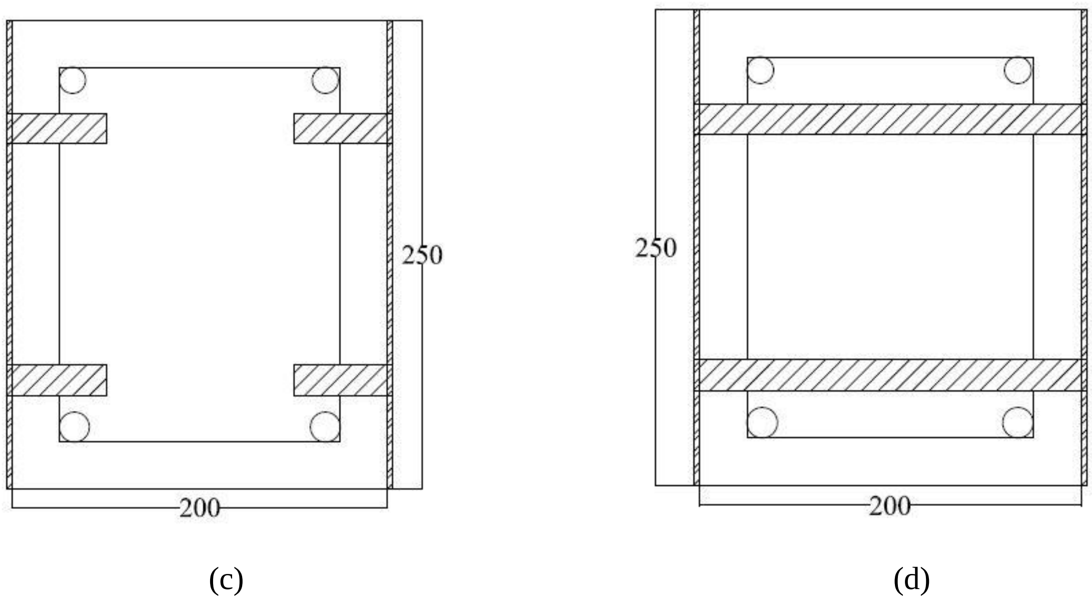

Figure 3.3 Cross section (a) control beam (b) 25 mm depth connector (c) 50 mm depth connector (d) 200 mm depth connector

3.2 Study Variables

Dependent variable: Failure load, maximum deflection, steel plate and longitudinal reinforcement bar strain

Independent variable: Variables which affects the shear strengthening of structural members.

- Width of steel plates
- Depth of connector

Beam dimensions, grade of concrete and strength of reinforcing steel and steel plates, number of connectors on a single steel plate and location of connectors are taken as a controlled variable, which was taken as constant.

3.3 Finite element modeling

The proposed strengthened model was introduced into nonlinear finite element model ABAQUS 6.14-1, which allows for nonlinear analysis of reinforced concrete beams, and both geometric and material nonlinearity.

3.3.1Geometric modeling

Concrete model

Concrete element was modeled as 8-noded linear hexahedral brick element with reduced integration and hourglass control (C3D8R) was used. This type of element has the capability of high convergence and reduces the computation time.

Reinforcing steel model

Reinforcement bar can be defined by three dimensional truss elements with linear shape function (T3D2). The elements were meshed the same approximate maximum size used in the beam part.

Structural plate model

Structural plate was modeled as a shell element (S4R) 4- node general purpose shell which is linear, finite membrane strain, reduced integration and suitable for wide range of application, uses to account the influence of shear flexibility for modeling thick shells.

Loading and supporting plates model

Supporting and loading plates that transfer the reaction and loads from to the concrete elements are modeled as solid element similar to the concrete. The approximate mesh size used is similar that used for concrete and reinforcing steel bar.

3.3.2 Material modeling

3.3.2.1 Concrete

3.3.2.1.1 Elastic behavior

The elastic behavior was modeled as linear and isotropic, standard values of modulus of elasticity of each concrete according to its grade and according to EBCS EN 1992-1-1: 2013.its value was calculated using the relation presented in equation 3.1.

$$E_{cm} = 22\left(\frac{f_{cm}}{10}\right)^{0.3} \qquad 3.1$$

Where $f_{cm} = f_c + 8$, f_{cm} is the mean compressive strength of concrete

To completely define the elastic property poisson's ratio should have to define. From different literature poission's ratio of concrete is in the ranges of 0.15-0.2. In this study a value of 0.18 for poission's ratio was chosen.

3.3.2.1.2 Damage plasticity model

In order to describe strength with the triaxial stress as input to finite element program ABAQUS, a set of five parameters are required to completely describe the plastic behavior of concrete; dilation angle (ψ), eccentricity (ε), f_{bo}/f_{co}, K_c, and viscosity parameter, the default values are preferred to be used by the ABAQUS and its vales are given on **Table 3.2**.

Table 3-2 CDP parameter

Dilation angle (ψ)	Eccentricity (ε)	f_{bo}/f_{co}	K_c	viscosity parameter
36^0	0.1	1.16	0.667	0.001

3.3.2.1.3 Compressive behavior

Concrete compressive behavior is input to the ABAQUS by applying the standard equation in EBCS EN 1992-1-1:2013 shown in equation 3.2

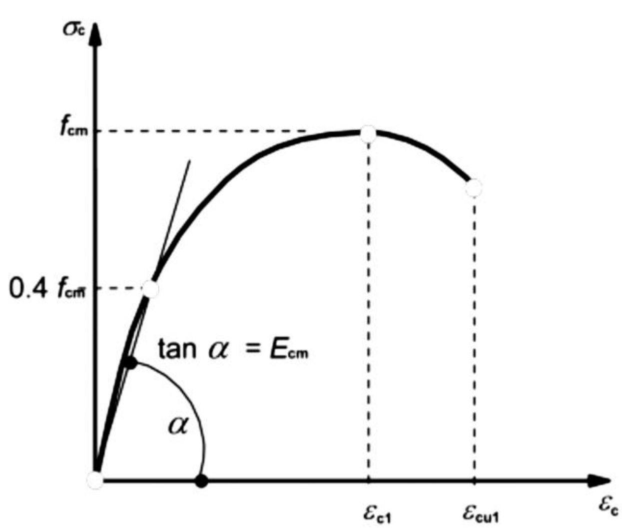

Figure 3.4 Compression Stress-Strain relation for concrete

$$\sigma_c = f_{cm} \frac{k\eta - \eta^2}{1 + (k - 2)\eta} \quad 3.2$$

Where:- $\eta = \varepsilon_c / \varepsilon_{c1}$

And $\varepsilon_{c1} = 0.7(fcm)^{0.31}$, is strain at peak stress according to to EBCS EN 1992-1-1:2013

k=$1.05 E_{cm} . \varepsilon_{c1} / f_{cm}$, k is factor

E_{cm} is secant modulus

3.3.2.1.4 Tensile behavior

Since tensile stiffening affects the result of the analysis and this are considered by using Wang & Hsu formula for the weakening function.

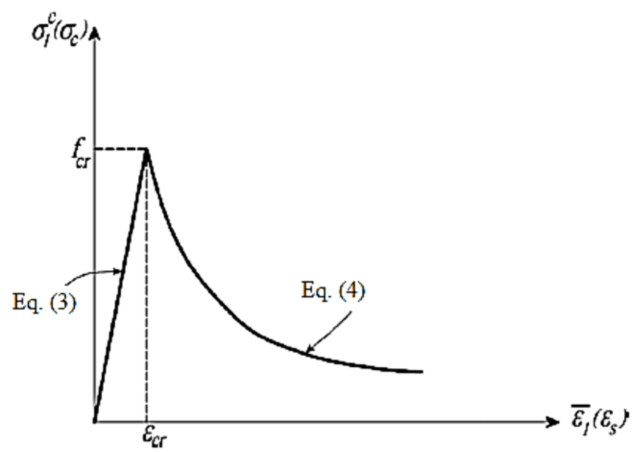

Figure 3.5 Tensile Stress-Strain relation for concrete

$$\sigma_t = E_{cm}\varepsilon_t \qquad for\ \varepsilon_t \leq \varepsilon_{cr} \quad 3.3$$

$$\sigma_t = f_{ctm} \left(\frac{\varepsilon_{cr}}{\varepsilon_t}\right)^{0.4} \qquad for\ \varepsilon_t > \varepsilon_{cr} \quad 3.4$$

For a cracked section a bilinear approach for the stress-crack opening relation is considered using model code 2010.

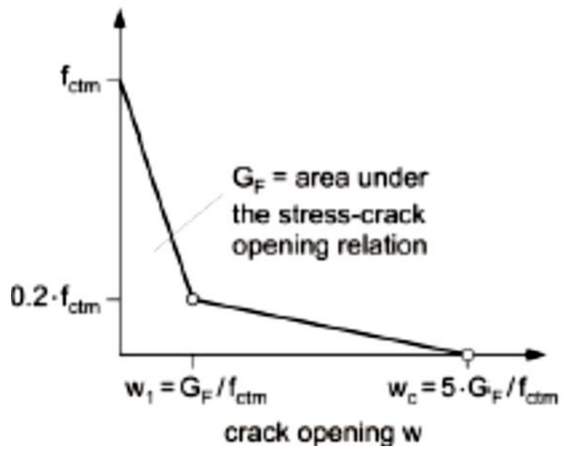

Figure 3.6 Tensile stress verses crack opening relation

$$\sigma_t = f_{ctm}\left(1 - 0.8\frac{w}{w_1}\right) \qquad for\ w \leq w_1 \qquad 3.5$$

$$\sigma_t = f_{ctm}\left(0.25 - 0.05\frac{w}{w_1}\right) \qquad for\ w_1 < w \leq w_c \qquad 3.6$$

Where: - w is crack opening

$$w_1 = \frac{GF}{f_{ctm}} \qquad where\ \sigma_t = 0.2 f_{ctm}$$

$$w_c = 5\frac{GF}{f_{ctm}} \qquad where\ \sigma_t = 0$$

$GF = 73. {f_{cm}}^{0.18}$, GF is the fracture energy (N/mm)

$f_{ctm} = 0.3. {f_{cm}}^{\frac{2}{3}}$, f_{ctm} is the tensile strength of concrete under uniaxial stress in (MPa)

ε_{cr} is the strain at concrete cracking

ε_t is the strain at any point after peak

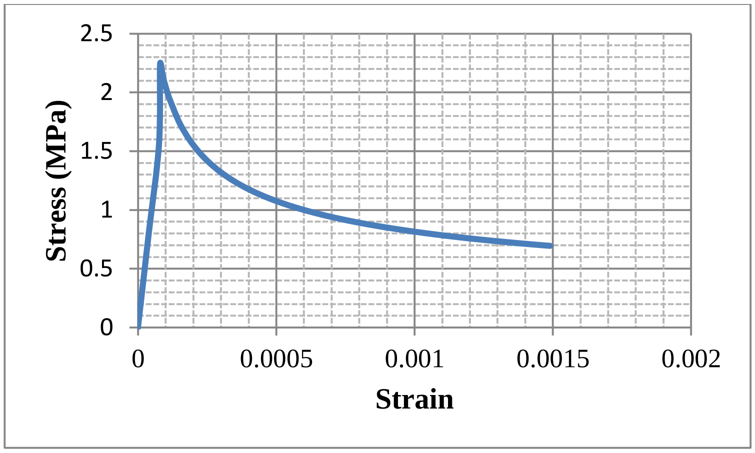

Figure 3.7 Tensile stress - strain relation for C20/25 concrete

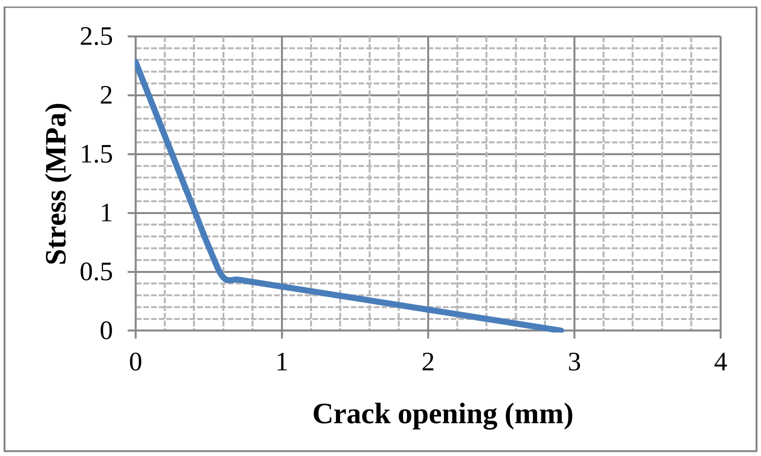

Figure 3.8 Stress and crack opening relation for C20/25 concrete

3.3.2.2 Reinforced bar, steel plate and embedded connector property

Reinforcement, typically steel bars are a ductile high strength material that have a ribbed surface to produce an improved bond with concrete. Unlike concrete, steel is a homogenous material that is taken to behave the same in tension as in compression. The idealized stress strain curve elastic perfectly plastic is presented in **Figure 3.9**. Where the elastic behavior is well delimited and it lasts until the yielding strength, f_y, is reached and after the material behaves plastic, deformations being irreversible. This propriety also used for steel plates and embedded connectors.

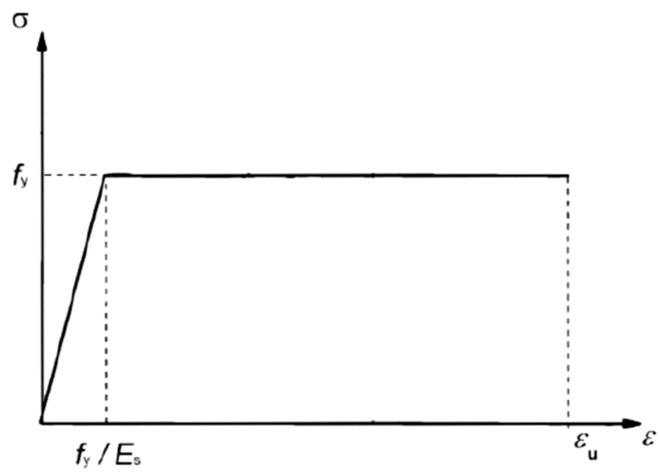

Figure 3.9 Stress strain relation for reinforcing steel and steel plate

$$f_s = E_s \varepsilon_s \qquad \varepsilon_s \leq \varepsilon_y \qquad 3.7$$

$$f_s = f_y \qquad \varepsilon_s \geq \varepsilon_y \qquad 3.8$$

3.3.3 Finite element mesh

When undertaking any finite element analysis, and in particular a nonlinear analysis, it is extremely important to choose suitable elements and an associated mesh in order to obtain a satisfactory solution to the problem. As the method is approximate, it is important to have a good understanding of the consequences of the assumptions when choosing the element types used and size of mesh. This allows the effects of the approximation to be minimized within the solution. In this study mesh density was investigated for the model, and a mesh size of 25mm was chosen in each direction. In addition, the selected mesh size maintains a balance between computational time and accuracy of results.

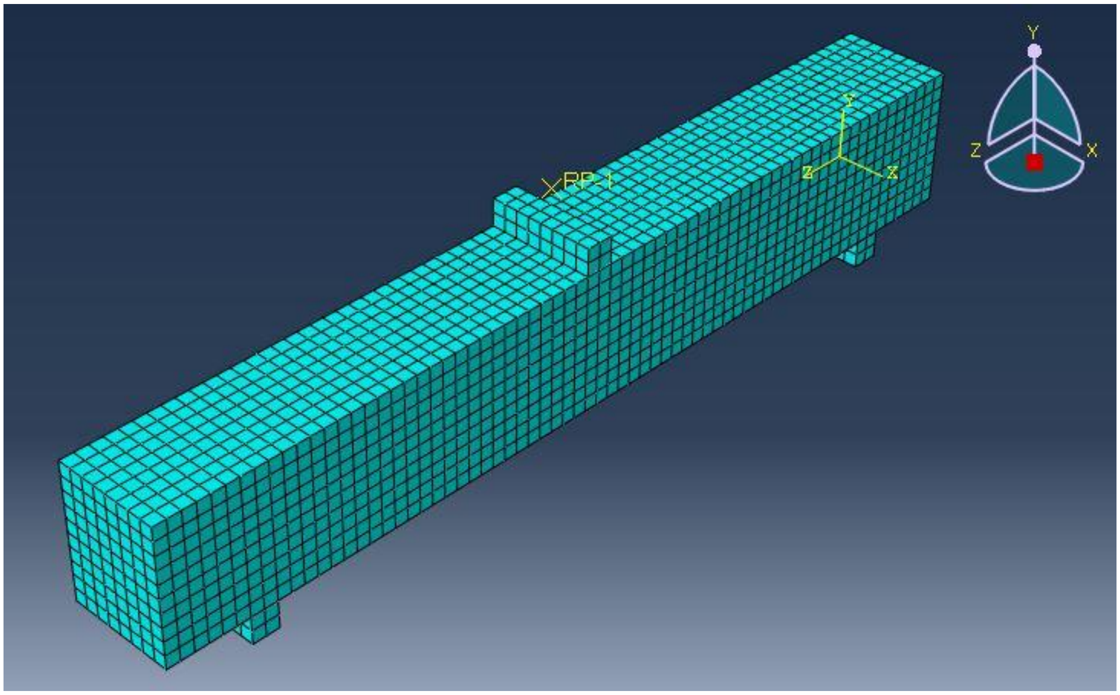

(a)

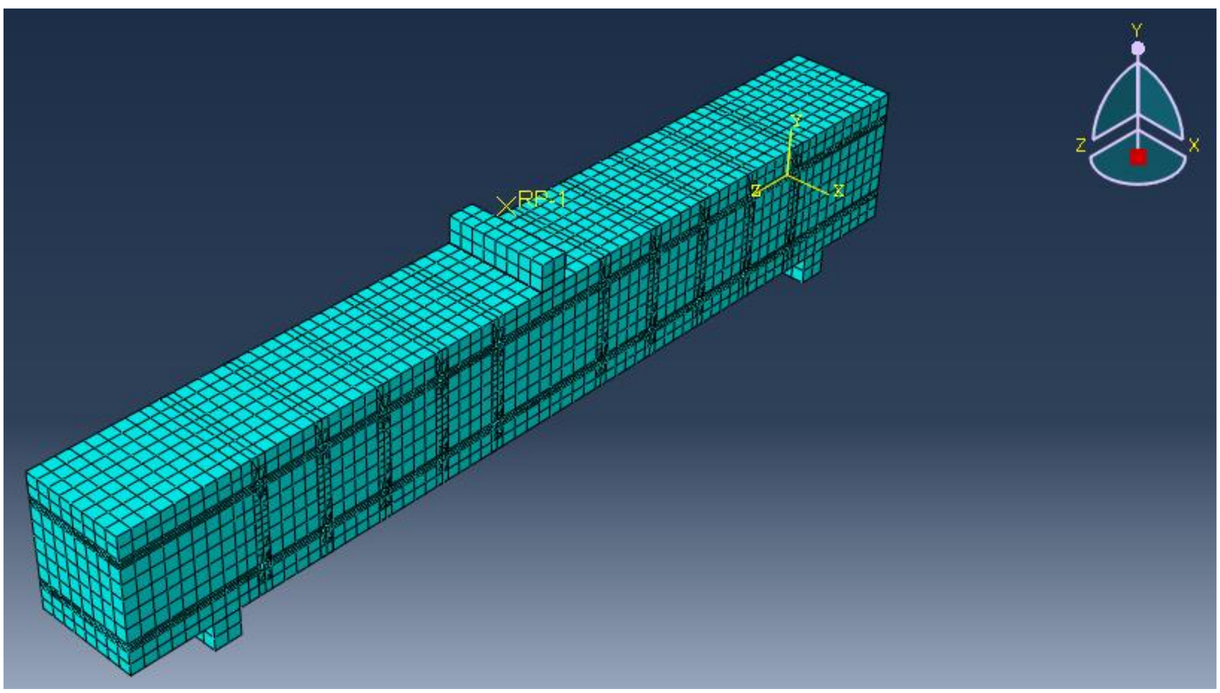

(b)

Figure 3.10 Element mesh, (a) mesh for control beam, (b) mesh for beams with steel plate

3.3.4 Interaction

In this study, truss elements were used to represent the reinforcement and these was embedded in the “host” continuum solid elements. Embedded means that the translation degree of freedom at the nodes of the embedded element are eliminated, and become constrained to corresponding interpolated value in the host continuum element.

For modeling bond area between the strengthening plate section with the concrete surface of the beam, as well as the embedded connector and the concrete surface, tie constraints were utilized. Tie constraints are used to tie together two surfaces for the duration of a simulation where each node on the slave surface is constrained to have the same motion as the point on the master surface to which it is closest. For a structural analysis, this means the translational degrees of freedom are constrained. In our case, the steel plate and embedded connectors acted as the master surfaces while the concrete surface of the beam acted as the slave surface.

To avoid stress concentration within the concrete beam, the reaction forces are transferred the beam through plates defined as discrete rigid bodies. Plate transferring reactions from the support are connected to the beam specimen using “tie” option, which means that parts cannot be disconnected during loading.

3.3.4 Boundary conditions

The beams were simply supported with 1.3 m clear distance between the supports. The beam was restrained on one side of the support along y direction only (roller support model) but on the other side support the beam was restrained in two directions along y and z-direction (pin support model). The plate at mid span used to apply load was restrained in y-direction and the load is applied with a coupled mechanism.

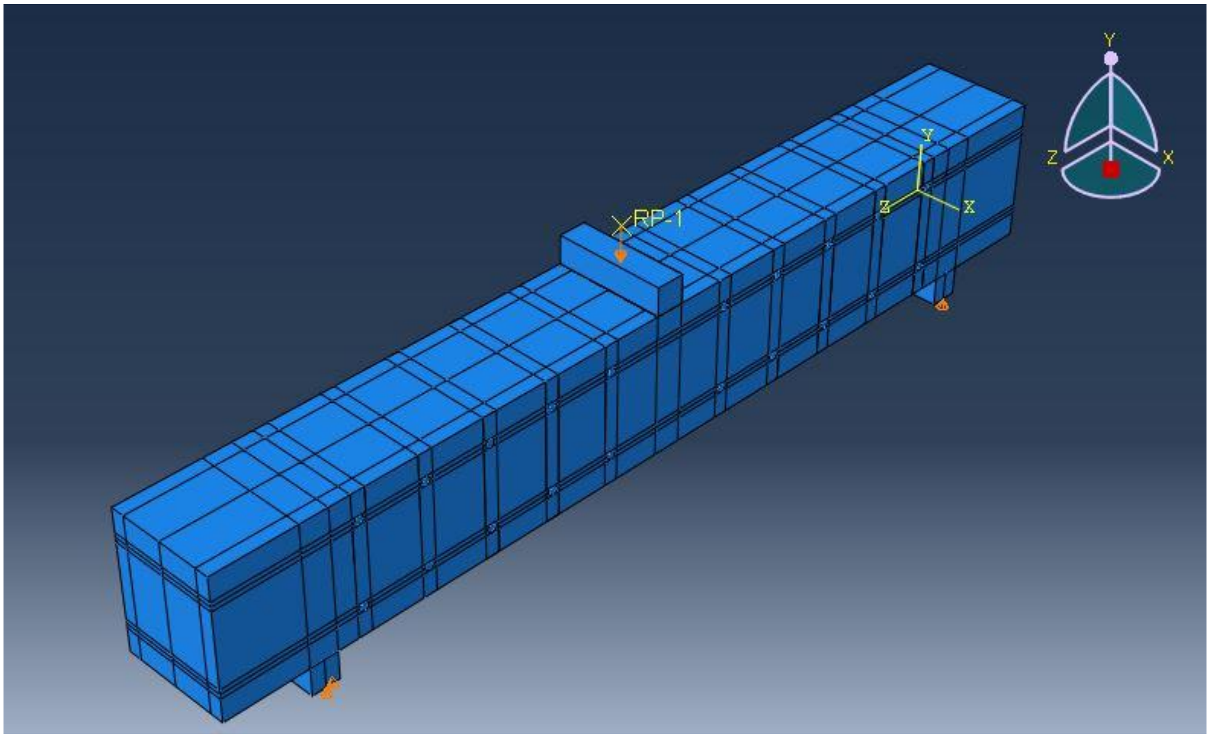

Figure 3.11 Boundary condition

3.4 Loading and Interpretation of Results

Displacement controlled load was induced to capture the post-peak response of the reinforced concrete beams. The displacement was applied to the beam as a time step type of loading. And as a result the nonlinear finite element software gives respective responses of every increment. In this research to compare the spacemen results load and deflection of mid span, strain of plates and strain of main reinforcement was taken.

CHAPTER FOUR

RESULT AND DISCUSSION

4.1 Validation of Finite Element Analysis

In order to check the validation of Finite Element Analysis Embedded connector of steel plates were analyzed with the experimental and numerical analysis of previous researches. The verification was done by comparing the maximum load and maximum deflection obtained from ABAQUS output to that of experimental ones.

Two specimens were used for verification. The specimens were from Md. Ashraful Alam *et.*al, CB which was the control beam of length 2,300mm, 300mm depth and 150mm width, BSC20 and BSC25 is the same size with control beam and had 20mm and 25mm width plate respectively, which was embedded to beam at a depth of 25mm by 16mm diameter connector. BSC30 were a beam having 30mm steel plate width with connector diameter of 20mm and 25mm depth.

On the basis of the experimental response of reinforced concrete members shear strengthening using embedded connector system is promising, this gain is higher as the width of steel plate increases. Furthermore, it is recommended for future investigations to use different arrangement of steel plates or increase the number of connectors used for single plate, which might help reduce the load carried by each connector.

Table 4-1 Summary of Results from Journal, All Beams

Specimen	Failure load (kN)		Variation %	Deflection(mm) at maximum kN load	
	Experimental	Numerical		Experimental	Numerical
CB	155.9	187	19.95	11.54	7.84
BSC20	178.6	184.8	3.47	11.79	8.08
BSC25	189.6	185.2	2.32	12.01	7.76
BSC30	193.4	188.9	2.33	11.43	8

4.1.1 Numerical Analysis Using ABAQUS

An analytical study was done according to the data given in the journal. The diagram of analyzed model is shown below.

Modeling of test beam (BSC20), concrete with characteristics strength with 31.385MPa was used to model concrete and embedded steel used to model reinforcement.

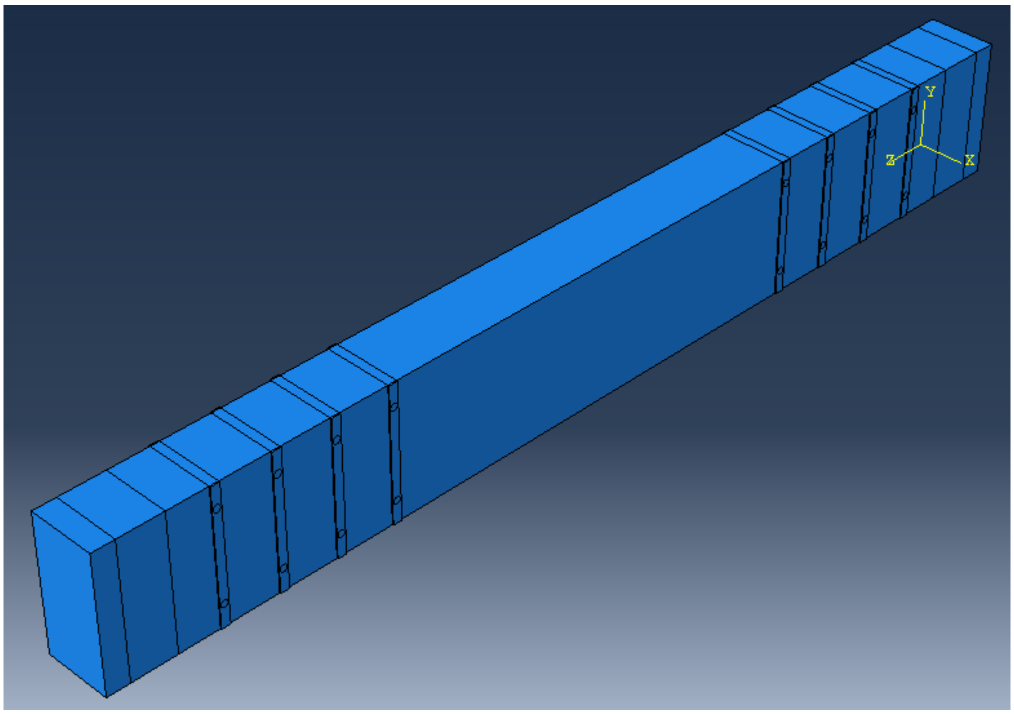

a)

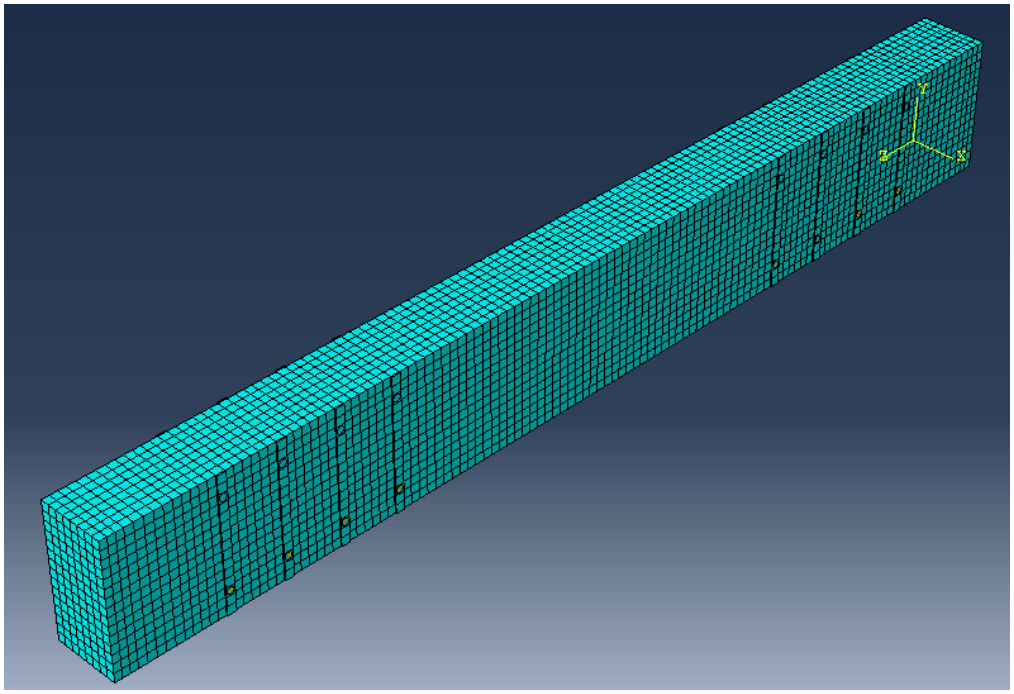

b)

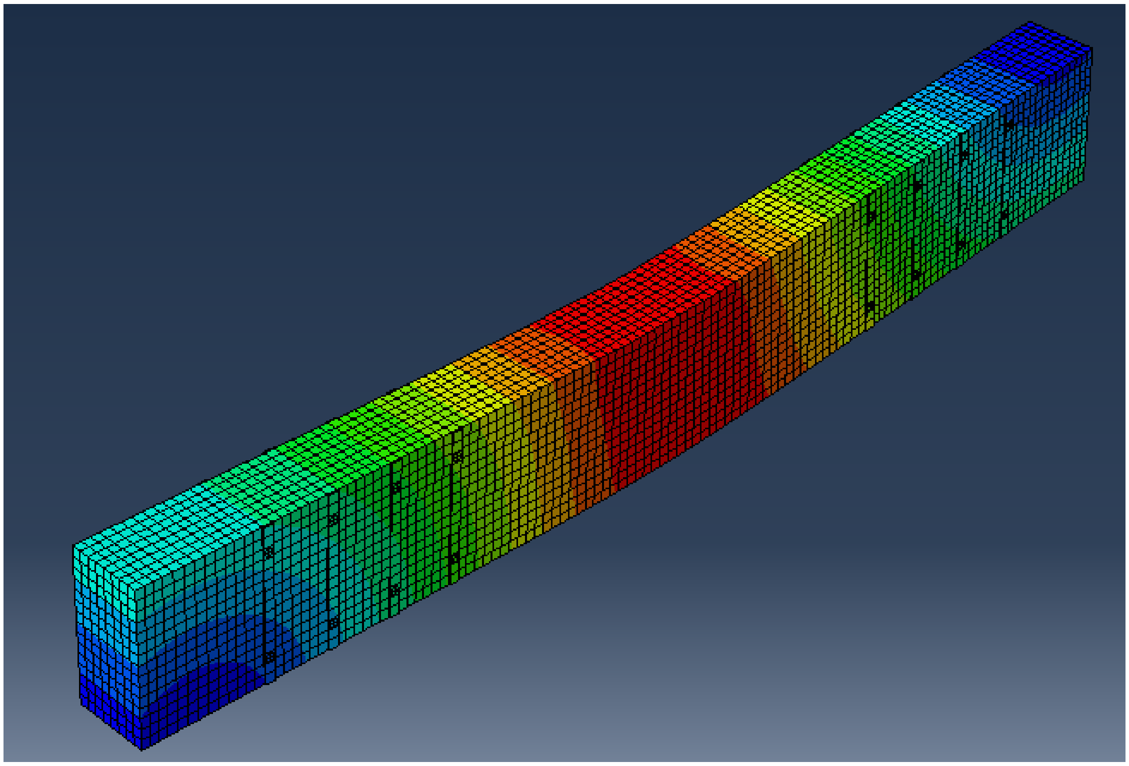

c)

Figure 4.1 BSC20 beam a) Model, b) Mesh and c) Deflection result

From the above **Figure 4.1 c)** the maximum deflection was at mid span and its value was about 13.98mm.

Table 4-2 Comparison with Journal result

Specimen	Journal data		ABAQUS result		Load variation (%)
	Maximum load (kN)	Deflection (mm)	Maximum load (kN)	Deflection (mm)	
CB	155.9	11.54	154.88	12.2	0.7
BSC20	178.6	11.79	171.09	13.98	4.4

From the above comparison, the result obtained from ABAQUS output is very much close to experimental result from the journal. Hence the software ABAQUS 6.14.1 is validated.

4.2 Finite Element Analysis output

For all beam types their result was discussed in the following sections. All specimens are effective in shear strengthening of reinforced concrete beams, were compared relative to control beam, which is a base line of strengthening techniques.

The results were discussed based on load versus mid span deflection and main reinforcement strain. Also the effect of steel plate width and embedded connector depth was discussed.

4.2.1 Load Carrying Capacity

The failure loads of all beams were compared with the control beam (CB) which was the base line for all the specimens. As stated on **Table 4.3** the failure load of control beam was 182.44kN measured at the mid span.

Under the first category which was connector depth of 25mm, W20D25, W25D25 and W30D25 beam fall with 227.85kN, 229.99kN, and 232.15kN load respectively. There were increases of the failure load 24.9%, 26.07% and 27.25% respectively when compared to a control beam.

The beam also categorized under the connector depth of 50mm were W20D50, W25D50 and W30D50 whose failure loads were 223.69kN, 233kN and 235.35kN respectively had an increase of carrying capacity of 22.61%, 27.72% and 29.01% respectively with the control beam.

The last category was connector depth of 200mm (throughout the width of the beam) had specimens W20D200, W25D200 and W30D200. Their failure loads were 240.57kN, 241.37kN and 248.52kN which have an increased load carrying capacity of 31.87%, 32.31% and 36.22% respectively with respect to that of control beam.

The steel plate-strengthened beams showed a regular increase in failure load with the increase in steel plate width. This indicated that the width of the steel plate and connector depth had a great effect on the shear capacity of the strengthened beam. The bigger width of the plate meant larger bonding area with the concrete surface and the larger connector depth provided more stiffness for the steel plate.

Table 4-3 Failure load

Connector Depth (mm)	Specimen	Failure Load (kN)	Deflection (mm)	Strain(μ)	
				Reinforcement	Plate
-	Control Beam	182.44	3.64	1,055.84	-
25	W20D25	227.85	5.45	1,332.78	544.67
	W25D25	229.99	5.47	1,339.52	299.65
	W30D25	232.15	5.03	1,364.75	301.51
50	W20D50	223.69	4.28	1,289.75	510.62
	W25D50	233.00	5.46	1,371.46	513.15
	W30D50	235.35	5.23	1,394.45	545.21
200	W20D200	240.57	5.17	1,455.74	199.27
	W25D200	241.37	5.59	1,473.09	159.00
	W30D200	248.52	5.52	1,499.66	171.67

Strain of reinforcing steel bar (longitudinal reinforcement), all beams bar strain was increased when compared with the control beams. For connector depth of 25mm, W20D25, W25D25 and W30D25 had strain increment of 26.23%, 26.87% and 29.26% respectively than the control beams.

Depth of connector having 50mm beams strain of reinforcement for W20D50, W25D50 and W30D50 had strain increment of 22.15%, 29.89% and 32.07% respectively than the control beams. And for connector depth of 200mm, W20D200, W25D200 and W30D200 had strain increment of 37.88%, 39.52% and 42.03% respectively than the control beam.

These indicates that the strengthening plates had good shear strength capacity, due to this the flexural stress occurred into the section becomes higher and higher.

From **Table 4-3** Strain of steel plates for 200mm depth connector showed a smaller value than other connector depths. This indicates that the depth of connector was restrained the elongation of plates and provide additional ductility to the beam.

4.2.2 Failure mode

Since the beams were designed intentionally to fail with shear failure. All beams were failed with shear failure before the yielding of longitudinal reinforcement. The failure load, failure mode and relative strength with the modeled and theoretical calculation (design of the beam) of control beam are described on **Table 4-4**. When the modeling and theoretical calculation were compared they had approximately the same failure load results, these indicates the modeling consistent with and theoretical calculation.

Shear capacity of reinforced concrete beams were constant as all beams had the same concrete and reinforcement properties and geometry. Whereas, shear resistance of plates was increasing with the width of steel plates and hole depth were increased. As discussed in **Table 4-4** all specimens had 22.71 kN to 33.04 kN shear resistance due to plate and connectors.

Table 4-4 Failure mode

Specimen	Failure Load (kN)	Calculated Failure load (kN)	Relative Strength with CB	$V_{plated\ beam}$ (kN)	V_c (kN)	V_{plate} (kN)	Failure Mode
CB	182.435	180.14	1.00	-	91.22	-	shear Failure
W20D25	227.854	-	1.25	113.93	91.22	22.71	shear Failure
W25D25	229.988	-	1.26	114.99	91.22	23.78	shear Failure
W30D25	232.149	-	1.27	116.07	91.22	24.86	shear Failure
W20D50	223.685	-	1.23	111.84	91.22	20.63	shear Failure
W25D50	232.998	-	1.28	116.50	91.22	25.28	shear Failure
W30D50	235.351	-	1.29	117.68	91.22	26.46	shear Failure
W20D200	240.572	-	1.32	120.29	91.22	29.07	shear Failure
W25D200	241.373	-	1.32	120.69	91.22	29.47	shear Failure
W30D200	248.515	-	1.36	124.26	91.22	33.04	shear Failure

From **Figure 4.2** the stress distribution of CB and other specimens were different in nature. CB stress distribution was continuous whereas specimen stress was discontinuous due to the presence of holes. This shows us using embedded connector steel plate prevents continuous crack propagation through the section.

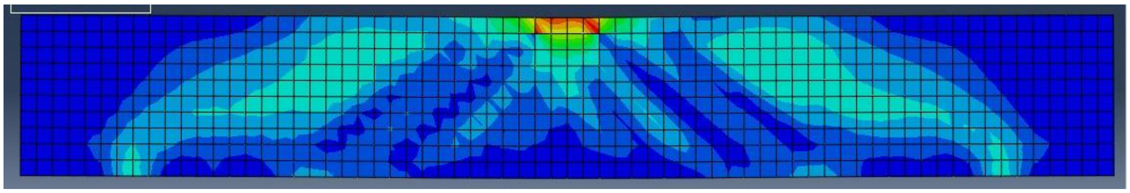

(a)

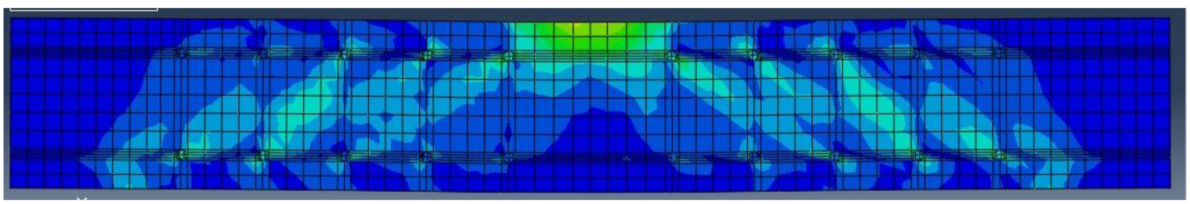

(b)

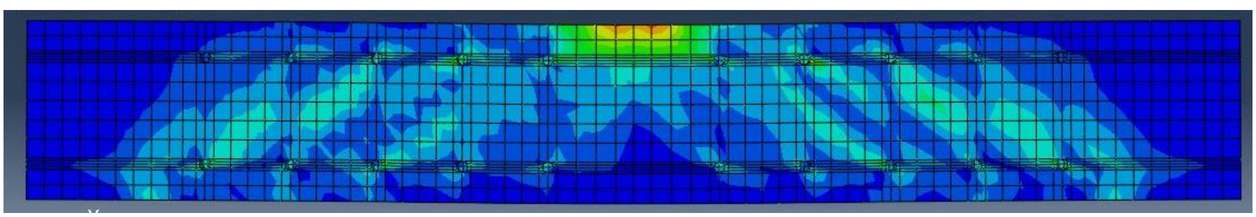

(c)

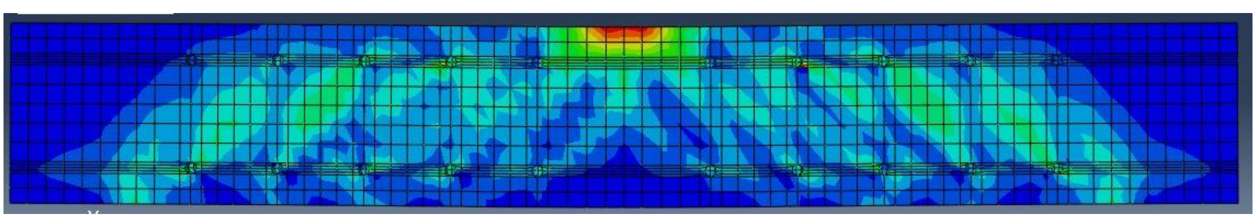

(d)

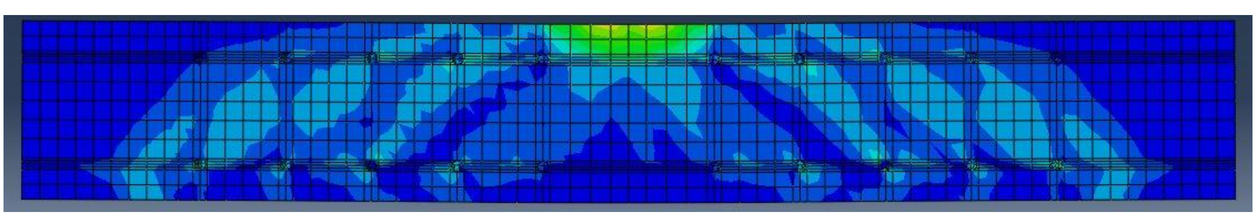

(e)

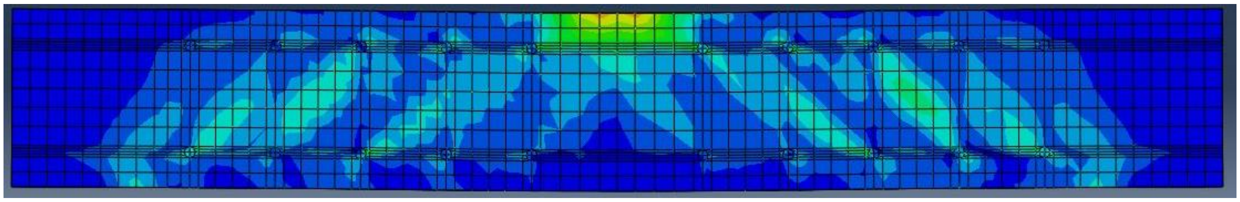

(f)

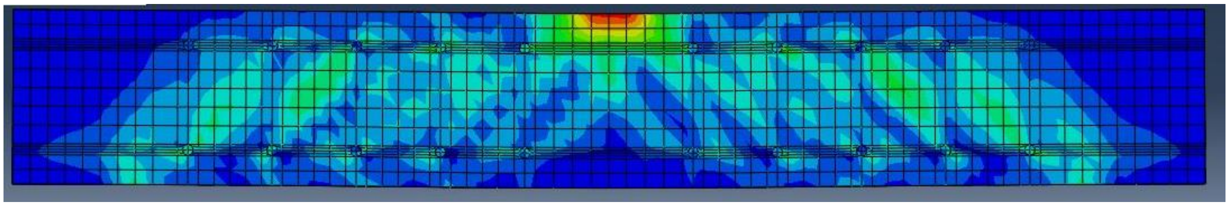

(g)

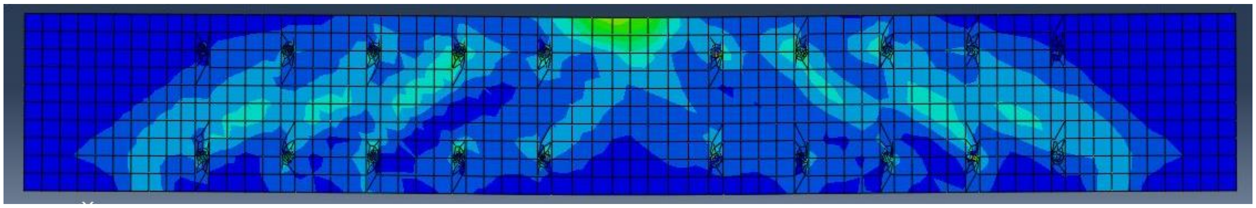

(h)

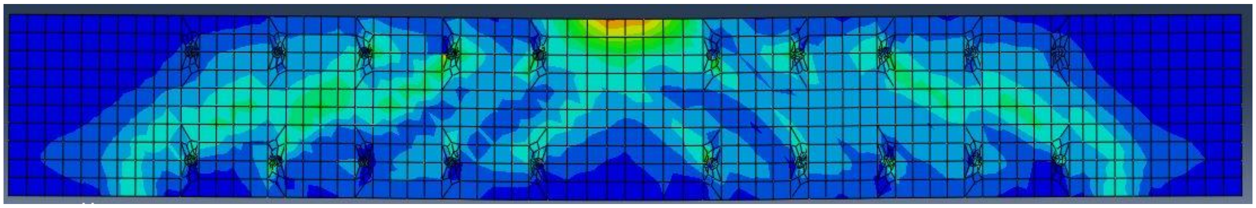

(i)

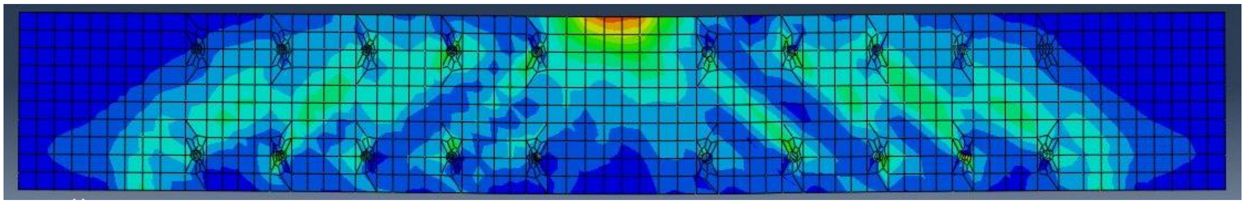

(j)

Figure 4.2 Failure mode (a) CB, (b) W20D25, (c) W25D25, (d)W30D25, (e) W20D50, (f)W25D50, (g)W30D50, (h)W20D200, (i)W25D200, (j)W30D200,

4.2.3 Load versus Deflection

Load and deflection of each specimen was discussed in the following section categorized by their respective depth and width. These results were taken at the mid span of the section to compare the specimens.

4.2.3.1 Effect of steel plate width

In the modeling of the specimens three different steel plate width were chosen, these were 20mm, 25mm and 30mm having the same thickness and length. Their corresponding effects are discussed on the following sections.

4.2.3.1.1 Connector Depth of 25mm

On this section, the effects of those three widths were compared each other which had load and deflection shown in **Figure 4.2** below. W20D25 had failure load of 227.84 kN at deflection of 5.45mm which is less than W25D25 and W30D25 having failure load of 229.99kN, 232.15kN at deflection of 5.47mm and 5.03mm respectively.

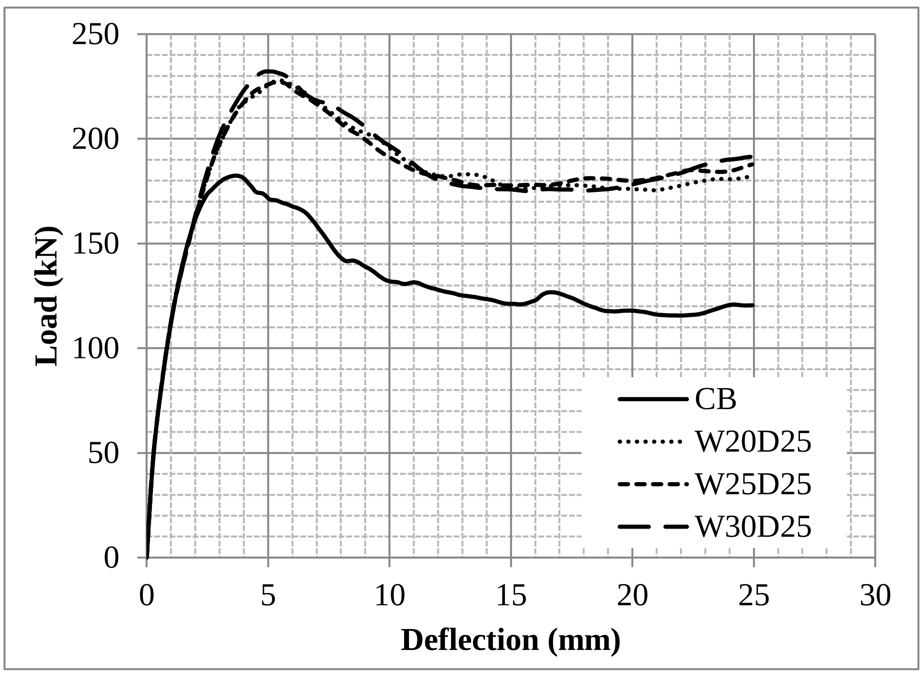

Figure 4.3 Load deflection curve for 25mm connector depth

4.2.3.1.2 Connector Depth of 50mm

For 50mm connector depth W25D50 had 233 kN failure load at a deflection of 5.46mm, which is 4.16% greater than W20D50 had 223.69 kN failure load at 4.28mm deflection. W30D50 had 235.35 kN failure loads at a deflection of 5.23mm greater than 5.21% compared to W20D50. This shows us an increase in the width of steel plate had effect on the load carrying capacity of the beam section.

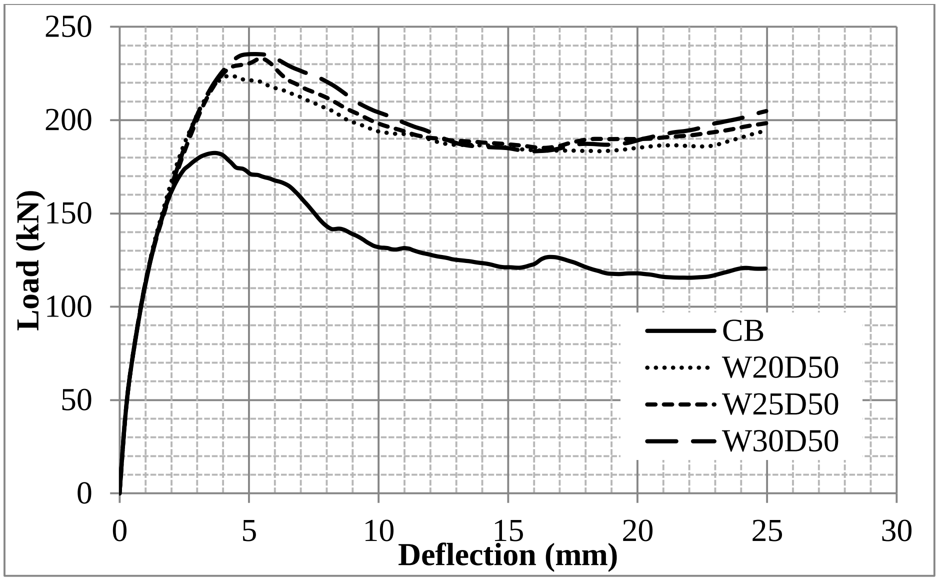

Figure 4.4 Load deflection curve for 50mm connector depth

4.2.3.1.3 Connector Depth of 200mm

From **Figure 4.5** three different width specimens of 200mm depth connector load and deflection had evaluated. Among them W30D200 had the largest load of 248.52kN with deflection 5.51mm, 3% larger than W20D200 whose load of 240.57 kN with 5.17mm deflection. W25D200 had almost the same load (241.37 kN) with W20D300 and 5.59mm deflection.

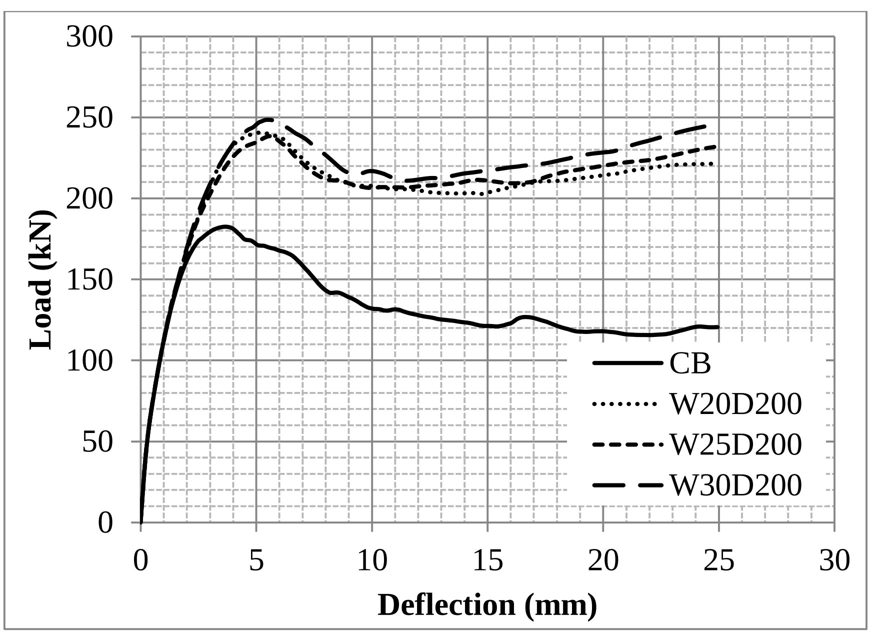

Figure 4.5 Load deflection curve for 200mm connector depth

From the above discussion on the effect of steel plate width depending on connector depth some beam had a slight change in the load carrying capacity of the section and some had significant increments on the failure load. This shows us the increase of the width of steel plate affects the load carrying capacity of the section.

This increment comes from; the first is due the increase in contact area of the plate to the concrete section which allows sufficient bond strength between steel plate and concrete beam. The second increase in the area of steel plate around the connector which provides additional tensile strength to the steel plate to resist shear stress.

4.2.3.2 Effect of Connector Depth

In the modeling of the specimens three different connector depths were chosen, these were 25mm, 50mm and 200mm (through the width of the beam). Their corresponding effects are drawn on the following Figure.

As shown on **Figure 4.6** the load deflection for every widths of the steel plate, when the depth of the embedded connector increases the failure load increases. Connector depth of 50mm and 200mm had the failure load increment of 1.3% and 5-7% respectively from 25mm depth of connector. This shows us the failure much become ductile. An increases depth of embedded connector provides additional load capacity that comes from stiffness of the section.

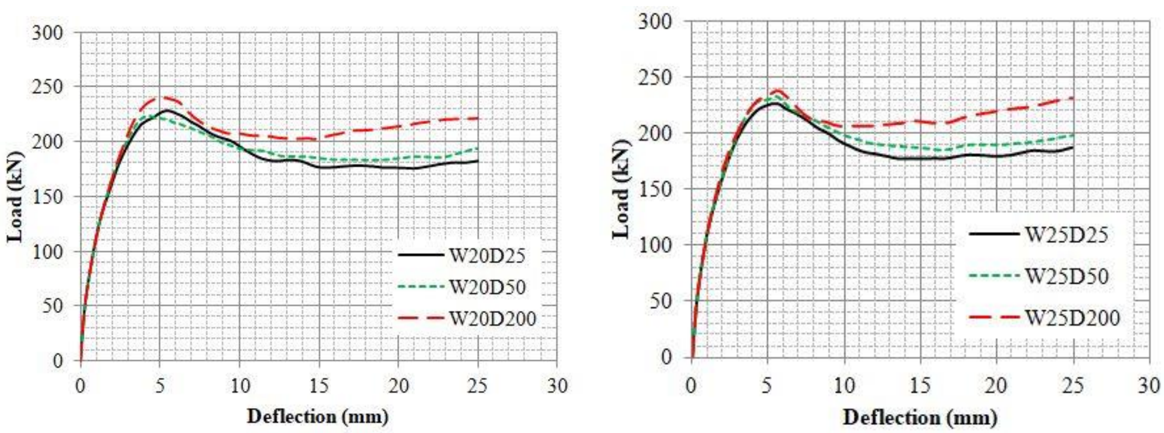

(a) (b)

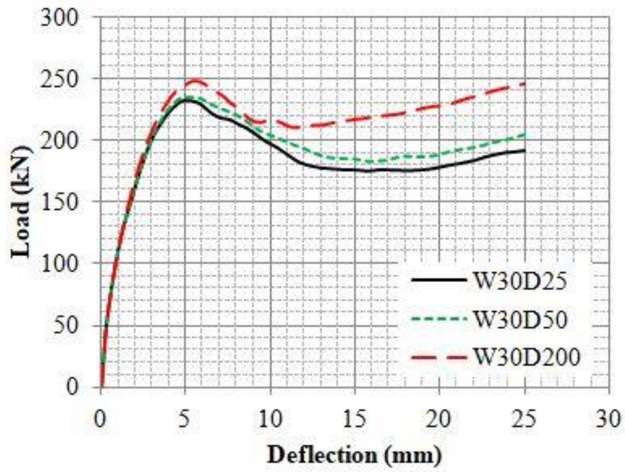

(c)

Figure 4.6 Effect of embedded connector depth, (a) for steel plate width 20mm, (b) for steel plate 25mm and (c) for steel plate 30mm

4.2.3.3 Effect of Hole Depth

Three beams were modeled and analyzed to know the effect of the holes on the load resistance relative to control beam. All holes had a diameter of 16mm which were the same as that of connector diameter and depth of hole depends on the depth of connector used on that of specimens. A connector hole having 25 mm depth supports 188.25 kN load which was 3% greater than control beam. A second beam which is modeled with a depth of 50mm had a 201.96 kN carrying capacity or 11% increasing of when compared to control beam. The last beam modeled was for hole 200mm (throughout width of the beam) had 182.92 kN failure load which is almost the same to control beam capacity which was 182.44 kN.

Holes with 25mm and 50mm depth had relatively higher load caring capacity as shown on **Figure 4.7**. These holes distribute or vanish the coming shear forces; as a result, the shear crack takes a time to pass along the holes. Also the presence of the hole provides energy to dissipate around the hole and these provide slower crack propagation in to the concrete section.

For 200mm hole has a smaller load carrying capacity when compared with hole size 25mm and 50mm these comes from the reduction of the core concrete and this generate instability on the structure. This modeled beam has approximately the same strength with the control beam, but ductile mode of failure when compared to CB. These comes from the hole affects the crack propagation in to the section.

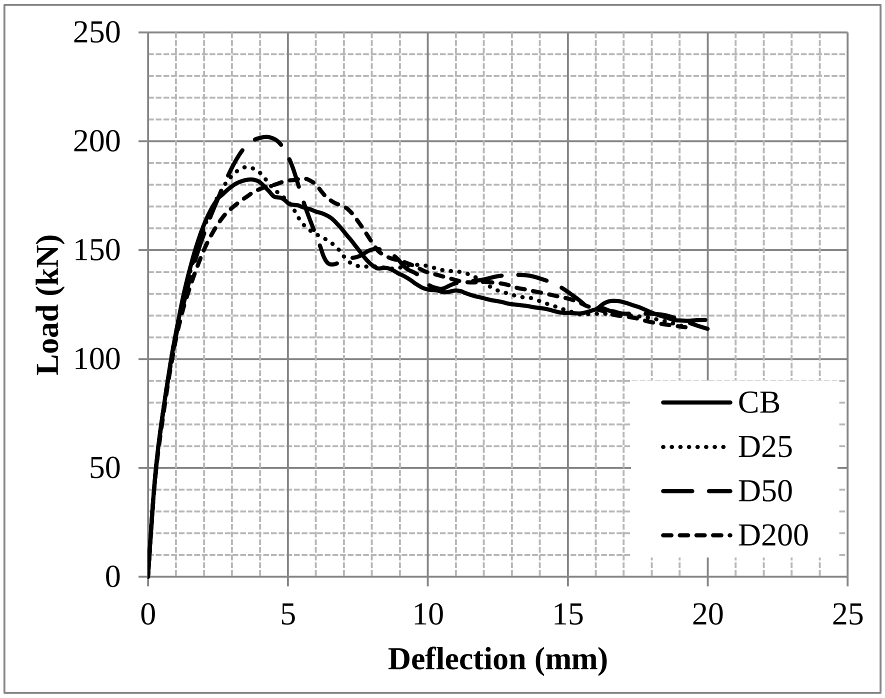

Figure 4.7 Load deflection curve for hole effect

CHAPTER FIVE

CONCLUSIONS AND RECOMMENDATIONS

5.1 Conclusions

Shear in the beam is primarily resisted by the stirrups provided as shear reinforcement. Beam members with insufficient stirrup bars require retrofitting in shear critical region, in order to enhance their shear strength.

In this research, different width of steel plate and connector depth were used to strengthen shear critical reinforced concrete beams. Software simulation programs were used to perform the effectiveness of strengthened beams. The relative efficiency of the various strengthening steel plate width and connector depth were examined. And widths of steel plate and connector depth have a positive role on shear capacity.

Result of software simulated beams shows that, all strengthened specimens were effective in shear improvement of a beam. On the study of the effect of width of steel plate depending on different depth of connector, for connector depth 25mm, 50mm and 200mm W30D25, W30D50 and W30D200 had failure load increment of 27.25 %, 29.01% and 36.22% respectively with respect to CB at 5.03 mm, 5.23mm and 5.52mm deflection which was efficient from other width of plates.

Hole drilling depth had difference failure load of beam, which was 3.19%, 10.7% and 0.26% for 25mm, 50mm and 20mm hole depths compared to CB. Which results 50mm hole depth without steel plate was most efficient.

Embedded connectors prevented premature debonding of steel plates between steel plates and concrete surface. The embedded connector for shear-strengthened beam of proposed design based on failure load W30D200 had maximum shear failure load with good ductile nature. This showed us from the width of steel plate and embedded connector depth taken on this research work W30D200 was most efficient.

5.2 Recommendations

Shear strengthening using embedded connector system is promising; more research is needed to verify the results of this study. Furthermore, it is recommended for future investigations:

- To use different arrangement of steel plates.
- Increase the number of connectors used for single plate, which might help reduce the load carried by each connector.
- To use different connector dimensions which affect the contact surface between concrete and steel plate.
- Different spacing of embedded connectors.
- To check the applicability for T- beams.
- Check for that of deep beams for shear strengthening.

To apply embedded connector steel plate for shear strengthening care should be considered: -

- Steel plates should be placed on the shear critical region of the beam.
- The selection of steel plate width and thickness.
- Drilled sections should fill with cementing material as much as possible to make good bond with existing structure.
- During drilling of a structural elements care should be done to protect internal reinforcement from any damage.
- Surface between the plates and concrete should be well cleaned and appropriate adhesive should be used.
- When retrofitting is done adequate support should be provided throughout the length of beam.
- Plastering of the steel plates should be done for aesthetic and corrosion effect.

REFERENCES

[1] O. Anil, N. Bulut, and M. Ayhan, "Strain distribution between ¨CFRP strip and concrete at strengthened RC beam against shear," *Structural Engineering and Mechanics*, vol. 41, no. 4, pp. 509–525, 2012.

[2] L. Ascione and L. Feo, "Modeling of composite/concrete interface of RC beams strengthened with composite laminates," *Composites Part B: Engineering*, vol. 31, no. 6-7, pp. 535–540, 2000.

[3] D. Baggio, K. Soudki, and M. Noel, "Strengthening of shear ¨critical RC beams with various FRP systems," *Construction and Building Material*, vol. 66, pp. 634–644, 2014.

[4] H. N. Garden and L. C. Hollaway, "An experimental study of the failure modes of RC beams strengthened with prestressed carbon composite plates," *Composites Part B: Engineering*, vol. 29, no. 4, pp. 411–424, 1998.

[5] J. Sim, C. Park, and D. Y. Moon, "Characteristics of basalt fiber as a strengthening material for concrete structures,"*Composites Part B: Engineering*, vol. 36, no. 6-7, pp. 504–512, 2005.

[6] B. Taljsten and L. Elfgren, "Strengthening of concrete beams for shear using CFRP materials: evaluation of different application methods," *Composites Part B: Engineering*, vol. 32, no. 2, pp. 87–96, 2000.

[7] J. Yao, J. G. Teng, and J. F. Chen, "Experimental study on FRPto-concrete bonded joints," *Composites Part B: Engineering*,vol. 36, no. 2, pp. 99–113, 2005.

[8] K. C. Panda, S. K. Bhattacharyya, and S. V. Barai, "Shear strengthening effect by bonded GFRP strips and transverse steel on RC T-beams," *Structural Engineering and Mechanics*, vol. 47, no. 1, pp. 75–98, 2013.

[9] W. Li and C. K. Y. Leung, "Shear span–depth ratio effect on behavior of RC beam shear strengthened with full-wrapping FRP strip," *Journal of Composites for Construction*, vol. 20, no. 3, p. 04015067, 2016.

[10] A. B. Shuraim, "Efficacy of CFRP configurations for shear of RC beams: experimental and NLFE," *Structural Engineering and Mechanics*, vol. 39, no. 3, pp. 361–382, 2011.

[11] T. C. Triantafillou and C. P. Antonopoulos, "Design of concrete flexural members strengthened in shear with FRP," *Journal of Composites for Construction*, vol. 4, no. 4, pp. 198–205, 2000.

[12] A. A. Jamal, S. A. Adi, A. H. Rami, and A. R. Hayder, "Shear strengthening of reinforced concrete beams using externally bonded aluminum alloy plates: An experimental study," *Construction and Building Materials*, vol. 128, pp. 24–37, 2016.

[13] A. Abu-Obeidah, R. A. Hawileh, and J. A. Abdalla, "Finite element analysis of strengthened RC beams in shear with aluminum plates," *Computers and Structures*, vol. 147, pp. 36–46, 2015.

[14] B. B. Adhikary and H. Mutsuyoshi, "Shear strengthening of reinforced concrete beams using various techniques," *Construction and Building Materials*, vol. 20, no. 6, pp. 366–373, 2006.

[15] Richard Andrew B. & Geoffrey Charles M., Strengthening of reinforced concrete beams in shear by the use of externally bonded steel plates (2005), www.sciencedirect.com

[16] Hiroshi M. & Bimal Babu A., Shear strengthening of reinforced concrete beams using various techniques, (2005), www.sciencedirect.com

[17] K. S. Panigrahi, A. Deb, and K. S. Bhattacharyya, "Modes of failure in shear deficient RC T-beams strengthened with FRP," *Journal of Composites for Construction*, vol. 20, no. 1, p. 04015029, 2016.

[18] ABAQUS 6.14 Analysis User's Guide Volume III: Materials

[19] ABAQUS 6.14 getting started with ABAQUS: interactive edition

[20] ABAQUS 6.14 analysis user's guide volume IV: elements

[21] Md. Ashraful Alam, Suliman A. Bakkar , Shahnawaz A. Onik, and Kamal N. Mustapha. "Embedded Connector in Severe Optimization of Steel Plate for." Hindawi, 2018: 1-12.

[22] EBCS EN 1992-1-1:2013: EBCS 2: Design of concrete structures.

APPENDICES

Appendix A: Design of beam

Dimension of beam and other specifications

- Total beam length = 1.7m
- Clear span of beam =1.3m
- Depth of beam= 250mm
- Width of beam = 200mm
- Concrete cover = 25mm
- Stirrups diameter = 6mm (out of shear span to prevent bond failure)
- Longitudinal bar in one row(bottom) =30mm (two number of bars)
- Longitudinal bar in one row(top) = 14mm (two number of bars)

Initial data's and Material strength

$$d' = 33mm$$

$$d = D - d' = 250 - 33 = 217mm$$

$$d2 = 32mm$$

Ratio of shear span to effective depth=$\frac{av}{d} = \frac{0.65}{0.209} = \mathbf{3.11}$ is a slender beam

Actual $\mathbf{A_s}$ (longitudinal tension bars) = 706.5 mm^2 (2ø30)

Actual $\mathbf{A_{s2}}$(longitudinal compression bars) = 200.96mm^2 (2ø16)

Concrete	Rebar
C-25	$S_{tension}$=500MPa
f'_c=20MPa	$S_{compression}$=500 MPa

$K_2 = 1.6 - \text{d} = 1.6 - 0.217 = 1.38$

$fct = 0.31(f'c)^{\frac{2}{3}} = 2.284\ MPa$

$\mathrm{K1} = 1 + 50 * \rho = 2$

$\mathrm{Vc} = 0.25 * \mathrm{fct} * \mathrm{k1} * \mathrm{k2} * \mathrm{b} * \mathrm{d} = 90.07\ \mathrm{KN}$

Back analysis of beam by using the actual specification of materials the maximum moment capacity of the beam

$Md, s = 90.92KNm$

$$M = \frac{PL}{4} \rightarrow P = \frac{4M}{L} = \frac{4 * 90.92}{1.3} = 279.75\ KN$$

Shear strengthening by percent (%) = $\frac{P}{2*Vc} * 100 = 121.98\ \%$

$$Kx = 0.5\{2.5 - \sqrt{2.5^2 - \left(\frac{4Msd}{0.32fc * b * d^2}\right)})\}$$

$$kx = 1.01 > Kx.lim = 0.448$$

The section is doubly reinforced section,

$$M1 = 0.8bd^2fc * Kx, lim(1 - 0.4Kx, lim) = 60.36MPa$$

$$As2 = \frac{M - M1}{fy(d - d2)} = 330.38mm^2$$

Design for steel plate, since the section does not have shear reinforcement the plate supports the remaining shear force.

$$V_{design} = V_{max}$$

$$V_{design} = V_{beam} - V_{plate}$$

$$V_{plate} = V_{max} - V_{beam}$$

$$Vst = \frac{A_{sw}Zfycot\theta}{s} = (A_{sw}0.9 * d * fy * cot\theta)/s$$

$$V_{plate} = 2A_{plate}f_y N$$

$$V_{plate} = \frac{A_{sw} * 0.9 * d * fy_{plate} cot\theta}{s_{plate}}$$

For the maximum width where the beam to be failed with shear is:

Force resistance due to moment = applied force to the structure

P= 279.75kN

$P_{cshear\ resistance}$ = 180.14kN

$V_{plate}(P_{resisted\ by\ plate})$ = P - $P_{cshear\ resistance}$ = 99.61kN

$$A_{sw} = \frac{V_{plate} * S_{plate}}{Z * cot\theta * f_{y,plate}}$$

- Where S_{plate} =120mm, Z=195.3mm, cot θ=1, f_{yplate} = 250MPa and V_{plate} = 99.61kN

$$A_{sw} = \frac{99.61 * 120}{195.3 * 1 * 250} = 122.39mm^2$$

- Where the thickness of the plate is 3mm

$$A_{sw} = t_{plate} * b_{plate} \rightarrow b_{plate} = \left(\frac{A_{sw}}{t_{plate}}\right)$$

$$b_{plate} = \frac{122.39}{3} = 40.78mm$$

- Therefore, to obtain pure shear failure the width of steel plate not more than 40.78mm

Appendix B: Input file for a reference CB model

*Heading

** Job name: ControlBeam Model name: CB

** Generated by: Abaqus/CAE 6.14-1

*Preprint, echo=NO, model=NO, history=NO, contact=NO

** PARTS

*Part, name="Bottom Rebar"

*End Part

*Part, name=RC

*End Part

*Part, name=Stirrups

*End Part

*Part, name=Support

*End Part

*Part, name="Upper rebar"

*End Part

** ASSEMBLY

*Assembly, name=Assembly

*Instance, name=RC-1, part=RC

*Node

*Element, type=C3D8R

*Nset, nset=_PickedSet2, internal, generate

*Elset, elset=_PickedSet2, internal, generate

** Section: Section-Concrete

*Solid Section, elset=_PickedSet2, material=Concrete,

*End Instance

*Instance, name=Stirrups-1, part=Stirrups

*Node

*Element, type=T3D2

*Nset, nset=_PickedSet2, internal, generate

*Elset, elset=_PickedSet2, internal, generate

** Section: Section-stirrups

*Solid Section, elset=_PickedSet2, material=Stirrups

*End Instance

*Instance, name=Stirrups-2, part=Stirrups

*Node

*Element, type=T3D2

*Nset, nset=_PickedSet2, internal, generate

*Elset, elset=_PickedSet2, internal, generate

** Section: Section-stirrups

*Solid Section, elset=_PickedSet2, material=Stirrups

*End Instance

*Instance, name=Support-1, part=Support

*Node

*Element, type=C3D8R

*Nset, nset=_PickedSet2, internal, generate

*Elset, elset=_PickedSet2, internal, generate

** Section: Section-Support

*Solid Section, elset=_PickedSet2, material=Support,

*End Instance

*Instance, name=Support-2, part=Support

*Node

*Element, type=C3D8R

*Nset, nset=_PickedSet2, internal, generate

*Elset, elset=_PickedSet2, internal, generate

** Section: Section-Support

*Solid Section, elset=_PickedSet2, material=Support,

*End Instance

** *Instance, name=Support-3, part=Support

*Node

*Element, type=C3D8R

*Nset, nset=_PickedSet2, internal, generate

*Elset, elset=_PickedSet2, internal, generate

** Section: Section-Support

*Solid Section, elset=_PickedSet2, material=Support,

*End Instance

*Instance, name="Upper rebar-1", part="Upper rebar"

*Node

*Element, type=T3D2

*Nset, nset=_PickedSet2, internal, generate

*Elset, elset=_PickedSet2, internal, generate

** Section: Section-Bottom Rebar

*Solid Section, elset=_PickedSet2, material="Bottom Rebar"

*End Instance

*Instance, name="Upper rebar-2", part="Upper rebar"

*Node

*Element, type=T3D2

*Nset, nset=_PickedSet2, internal, generate

*Elset, elset=_PickedSet2, internal, generate

** Section: Section-Bottom Rebar

*Solid Section, elset=_PickedSet2, material="Bottom Rebar"

*End Instance

*Instance, name="Bottom Rebar-1", part="Bottom Rebar"

*Node

*Element, type=T3D2

*Nset, nset=_PickedSet2, internal, generate

*Elset, elset=_PickedSet2, internal, generate

** Section: Section-Bottom Rebar

*Solid Section, elset=_PickedSet2, material="Bottom Rebar"

*End Instance

*Instance, name="Bottom Rebar-2", part="Bottom Rebar"

*Node

*Element, type=T3D2

*Nset, nset=_PickedSet2, internal, generate

*Elset, elset=_PickedSet2, internal, generate
** Section: Section-Bottom Rebar

*Solid Section, elset=_PickedSet2, material="Bottom Rebar"

*End Instance

*Instance, name=Stirrups-1-lin-2-1, part=Stirrups

*Node

*Element, type=T3D2

*Nset, nset=_PickedSet2, internal, generate

*Elset, elset=_PickedSet2, internal, generate

** Section: Section-stirrups

*Solid Section, elset=_PickedSet2, material=Stirrups

*End Instance

*Instance, name=Stirrups-1-lin-3-1, part=Stirrups

*Node

*Element, type=T3D2

*Nset, nset=_PickedSet2, internal, generate

*Elset, elset=_PickedSet2, internal, generate

** Section: Section-stirrups

*Solid Section, elset=_PickedSet2, material=Stirrups

*End Instance

*Instance, name=Stirrups-1-lin-4-1, part=Stirrups

*Node

*Element, type=T3D2

*Nset, nset=_PickedSet2, internal, generate

*Elset, elset=_PickedSet2, internal, generate

** Section: Section-stirrups

*Solid Section, elset=_PickedSet2, material=Stirrups

*End Instance

*Instance, name=Stirrups-2-lin-2-1, part=Stirrups

*Element, type=T3D2

*Nset, nset=_PickedSet2, internal, generate

*Elset, elset=_PickedSet2, internal, generate

** Section: Section-stirrups

*Solid Section, elset=_PickedSet2, material=Stirrups

*End Instance

*Instance, name=Stirrups-2-lin-3-1, part=Stirrups

*Node

*Element, type=T3D2

*Nset, nset=_PickedSet2, internal, generate

*Elset, elset=_PickedSet2, internal, generate

** Section: Section-stirrups

*Solid Section, elset=_PickedSet2, material=Stirrups

*End Instance

*Instance, name=Stirrups-2-lin-4-1, part=Stirrups

*Node

*Element, type=T3D2

*Nset, nset=_PickedSet2, internal, generate

*Elset, elset=_PickedSet2, internal, generate

** Section: Section-stirrups

*Solid Section, elset=_PickedSet2, material=Stirrups

*End Instance

*Nset, nset=RF2, instance=Support-1

*Nset, nset=RF2, instance=Support-2

*Elset, elset=RF2, instance=Support-1

*Elset, elset=RF2, instance=Support-2

*Nset, nset=U2, instance=RC-1

*Nset, nset=_PickedSet103, internal, instance=Support-2

*Elset, elset=_PickedSet103, internal, instance=Support-2

*Nset, nset=_PickedSet174, internal 1,

*Nset, nset=_PickedSet188, internal, instance=Support-1

*Elset, elset=_PickedSet188, internal, instance=Support-1

*Nset, nset=_PickedSet201, internal

*Nset, nset=_PickedSet242, internal, instance=Stirrups-1, generate

*Nset, nset=_PickedSet242, internal, instance=Stirrups-2, generate

*Nset, nset=_PickedSet242, internal, instance="Upper rebar-1", generate

*Nset, nset=_PickedSet242, internal, instance=Stirrups-1-lin-4-1, generate

*Nset, nset=_PickedSet242, internal, instance="Bottom Rebar-1", generate

*Nset, nset=_PickedSet242, internal, instance=Stirrups-2-lin-3-1, generate

*Nset, nset=_PickedSet242, internal, instance=Stirrups-1-lin-2-1, generate

*Nset, nset=_PickedSet242, internal, instance="Upper rebar-2", generate

*Nset, nset=_PickedSet242, internal, instance=Stirrups-2-lin-2-1, generate

*Nset, nset=_PickedSet242, internal, instance="Bottom Rebar-2", generate

*Nset, nset=_PickedSet242, internal, instance=Stirrups-2-lin-4-1, generate

*Nset, nset=_PickedSet242, internal, instance=Stirrups-1-lin-3-1, generate

*Elset, elset=_PickedSet242, internal, instance=Stirrups-1, generate

*Elset, elset=_PickedSet242, internal, instance=Stirrups-2, generate

*Elset, elset=_PickedSet242, internal, instance="Upper rebar-1", generate

*Elset, elset=_PickedSet242, internal, instance=Stirrups-1-lin-4-1, generate

*Elset, elset=_PickedSet242, internal, instance="Bottom Rebar-1", generate

*Elset, elset=_PickedSet242, internal, instance=Stirrups-2-lin-3-1, generate

*Elset, elset=_PickedSet242, internal, instance=Stirrups-1-lin-2-1, generate

*Elset, elset=_PickedSet242, internal, instance="Upper rebar-2", generate

*Elset, elset=_PickedSet242, internal, instance=Stirrups-2-lin-2-1, generate

*Elset, elset=_PickedSet242, internal, instance="Bottom Rebar-2", generate

*Elset, elset=_PickedSet242, internal, instance=Stirrups-2-lin-4-1, generate

*Elset, elset=_PickedSet242, internal, instance=Stirrups-1-lin-3-1, generate

*Elset, elset=__PickedSurf173_S6, internal, instance=Support-3, generate

*Surface, type=ELEMENT, name=_PickedSurf173, internal

__PickedSurf173_S6, S6

*Elset, elset=__PickedSurf236_S4, internal, instance=Support-2, generate

*Elset, elset=__PickedSurf236_S6, internal, instance=Support-2, generate

*Surface, type=ELEMENT, name=_PickedSurf236, internal

__PickedSurf236_S4, S4

__PickedSurf236_S6, S6

*Elset, elset=__PickedSurf237_S6, internal, instance=RC-1, generate

*Surface, type=ELEMENT, name=_PickedSurf237, internal

__PickedSurf237_S6, S6

*Elset, elset=__PickedSurf238_S4, internal, instance=Support-3, generate

*Surface, type=ELEMENT, name=_PickedSurf238, internal

__PickedSurf238_S4, S4

*Elset, elset=__PickedSurf239_S6, internal, instance=RC-1, generate

*Surface, type=ELEMENT, name=_PickedSurf239, internal

__PickedSurf239_S6, S6

*Elset, elset=__PickedSurf240_S4, internal, instance=Support-1, generate

*Elset, elset=__PickedSurf240_S6, internal, instance=Support-1, generate

*Surface, type=ELEMENT, name=_PickedSurf240, internal

__PickedSurf240_S4, S4

__PickedSurf240_S6, S6

*Elset, elset=__PickedSurf241_S6, internal, instance=RC-1, generate

*Surface, type=ELEMENT, name=_PickedSurf241, internal

__PickedSurf241_S6, S6

** Constraint: Left support

*Tie, name="Left support", adjust=yes

_PickedSurf237, _PickedSurf236

** Constraint: Load

*Tie, name=Load, adjust=yes

_PickedSurf239, _PickedSurf238

** Constraint: couple

*Coupling, constraint name=couple, ref node=_PickedSet174, surface=_PickedSurf173

*Kinematic

** Constraint: embedded

*Embedded Element

_PickedSet242

** Constraint: right support

*Tie, name="right support", adjust=yes

_PickedSurf241, _PickedSurf240

*End Assembly

** MATERIALS

*Material, name="Bottom Rebar"

*Density

7.8e-06,

*Elastic

200000., 0.3

*Plastic

500., 0.

*Material, name=Concrete

*Density

2.4e-06,

*Elastic

28960.4, 0.18

*Concrete Damaged Plasticity

36., 0.1, 1.16, 0.667, 0.001

*Concrete Compression Hardening

12.5, 0.

14.3457, 0.000104646

17.5944, 0.000192467

20.184, 0.000303049

22.1684, 0.000434528

23.5957, 0.000585243

24.5092, 0.000753699

24.9478, 0.000938557

25., 0.00103547

24.9463, 0.00113861

24.5367, 0.00135275

23.7474, 0.00158

22.6046, 0.00181946

21.1321, 0.00207031

19.3515, 0.00233179

17.2826, 0.00260324

14.9435, 0.002884

13.6779, 0.0030277

*Concrete Tension Stiffening

2.24046, 0.

2.04915, 0.0001

1.96537, 0.000111

1.95508, 0.000112467

1.74843, 0.0001487

1.60239, 0.000184933

1.49171, 0.000221167

1.40388, 0.0002574

1.33184, 0.000293633

1.27127, 0.000329867

1.21936, 0.0003661

1.17419, 0.000402333

1.13438, 0.000438567

1.09893, 0.0004748

1.06707, 0.000511033

1.03823, 0.000547267

1.01194, 0.0005835

0.98785, 0.000619733

0.965651, 0.000655967

0.945106,   0.0006922

0.926013, 0.000728433

0.908205, 0.000764667

0.891542,   0.0008009

0.875901, 0.000837133

0.861181, 0.000873367

0.847291,   0.0009096

0.834156, 0.000945833

0.821706, 0.000982067

0.809884,   0.0010183

0.798636, 0.00105453

0.787917, 0.00109077

0.777684,   0.001127

0.767903, 0.00116323

0.758539, 0.00119947

0.749562,   0.0012357

0.740947, 0.00127193

0.732669, 0.00130817

0.724706,   0.0013444

0.717037, 0.00138063

0.709645, 0.00141687

0.702514,   0.0014531

0.695627, 0.00148933

0.693644,   0.0015

*Concrete Compression Damage

0., 0.

0., 0.000104646

0., 0.000192467

0., 0.000303049

0., 0.000434528

0., 0.000585243

0., 0.000753699

0., 0.000938557

0., 0.00103547

0.00214608, 0.00113861

0.0185334, 0.00135275

0.0501036,   0.00158

0.095814, 0.00181946

0.154715, 0.00207031

0.22594, 0.00233179

0.308698, 0.00260324

0.402262,   0.002884

0.452886,   0.0030277

*Concrete Tension Damage

0.   0.

0.102865,   0.0001

0.139544,   0.000111

0.14405, 0.000112467

0.23452,   0.0001487

0.298461, 0.000184933

0.346914, 0.000221167

```
0.385369,   0.0002574
 0.41691, 0.000293633
0.443426, 0.000329867
0.466151,   0.0003661
0.485928, 0.000402333
0.503358, 0.000438567
 0.51888,   0.0004748
0.532826, 0.000511033
0.545453, 0.000547267
0.556961,   0.0005835
 0.56751, 0.000619733
0.577229, 0.000655967
0.586224,   0.0006922
0.594583, 0.000728433
0.602379, 0.000764667
0.609675,   0.0008009
0.616522, 0.000837133
0.622967, 0.000873367
0.629048,   0.0009096
0.634799, 0.000945833
0.640249, 0.000982067
0.645425,   0.0010183
 0.65035, 0.00105453
0.655043, 0.00109077
0.659523,    0.001127
0.663805, 0.00116323
 0.667905, 0.00119947
 0.671835,   0.0012357
 0.675606, 0.00127193
 0.679231, 0.00130817
 0.682717,   0.0013444
 0.686074, 0.00138063
 0.689311, 0.00141687
 0.692433,   0.0014531
 0.695448, 0.00148933
 0.696316,      0.0015
*Material, name=Plate
*Density
 7.8e-06,
*Elastic
200000., 0.3
*Plastic
250., 0.
300., 0.01
*Material, name=Stirrups
*Density
 7.8e-06,
*Elastic
200000., 0.3
*Plastic
250., 0.
300., 0.01
```

*Material, name=Support

*Density

7.8e-06,

*Elastic

200000., 0.3

*Plastic

800., 0.

1000., 0.01

*Material, name="Upper Rebar"

*Density

7.8e-06,

*Elastic

200000., 0.3

*Plastic

420., 0.

500., 0.01

** BOUNDARY CONDITIONS

** Name: BC-2 Type: Displacement/Rotation

*Boundary

_PickedSet103, 2, 2

_PickedSet103, 3, 3

** Name: BC-3 Type: Displacement/Rotation

*Boundary

_PickedSet188, 2, 2

** STEP: Step-1

*Step, name=Step-1, nlgeom=YES, inc=10000

*Static

0.01, 5., 6e-06, 0.1

** BOUNDARY CONDITIONS

** Name: BC-4 Type: Displacement/Rotation

*Boundary

_PickedSet201, 2, 2, -40.

** OUTPUT REQUESTS

*Restart, write, frequency=0

** FIELD OUTPUT: F-Output-1

*Output, field

*Node Output

CF, RF, U

*Element Output, directions=YES

DAMAGEC, DAMAGET, LE, PE, PEEQ, PEMAG, S

*Contact Output

CDISP, CSTRESS

** HISTORY OUTPUT: RF2

*Output, history

*Node Output, nset=RF2

RF2,

** HISTORY OUTPUT: U2

*Node Output, nset=U2

U2,

** HISTORY OUTPUT: H-Output-1

*Output, history, variable=PRESELECT

*End Step